

Merging white dwarfs and SN Ia

L.R. Yungelson^{1*}, A. G. Kuranov²

¹*Institute of Astronomy of the Russian Academy of Sciences, 48 Pyatnitskaya Str., Moscow, Russia*

²*Sternberg Astronomical Institute, Moscow M.V. Lomonosov State University, 2 Lomonosov prosp., Moscow, Russia*

Accepted 2016 September 22, Received 2016 September 20; in original form 2016 July 25

ABSTRACT

Using population synthesis, we study a double-degenerate (DD) scenario for SNe Ia, aiming to estimate the maximum possible contribution to the rate of SNe from this scenario and the dependence of the delay-time distribution (DTD) on it. We make an extreme assumption that all mergers of super-Chandrasekhar pairs of CO white dwarfs (WDs) and mergers of CO WDs more massive than $0.47 M_{\odot}$ with hybrid or helium WDs more massive than $0.37 M_{\odot}$ produce SNe Ia. The models are parametrized by the product of the common envelope efficiency and the parameter of binding energy of stellar envelopes $\alpha_{ce}\lambda$, which we vary between 0.25 and 2. The best agreement with observations is obtained for $\alpha_{ce}\lambda=2$. A substantial contribution to the rate of SNe Ia is provided by the pairs with a hybrid WD. The estimated Galactic rate of SNe Ia is $6.5 \times 10^{-3} \text{ yr}^{-1}$ (for the mass of the bulge and thin disk equal to $7.2 \times 10^{10} M_{\odot}$), which is comparable to the observational estimate $(5.4 \pm 0.12) \times 10^{-3} \text{ yr}^{-1}$. The model DTD for $1 \leq t \leq 8 \text{ Gyr}$ satisfactorily fits DTD for SNe Ia in the field galaxies (Maoz et al. 2012). For this epoch, model DTD is $\propto t^{-1.64}$. At earlier and later epochs our DTD has a deficit of events, as in other studies. Marginal agreement with observational DTD is achieved even if only CO+CO WD with $M_1 \geq 0.8 M_{\odot}$ and $M_2 \geq 0.6 M_{\odot}$ produce SNe Ia. A better agreement of observed and model DTD may be obtained if tidal effects are weaker than assumed and/or metallicity of population is much lower than solar.

Key words: binaries: close — supernovae

1 INTRODUCTION

The exceptional role of SNe Ia in exploration of the riddles of the Universe is a result primarily of the fact that, with certain caveats, SNe Ia may be considered as ‘standard candles’ and serve as a measure of cosmic distance. The nature of SNe Ia is, however, still elusive. There exists only an agreement that they are related to the thermonuclear explosions of white dwarfs (WDs) (Hoyle & Fowler 1960).

The evolution of close binaries leading to formation of potential precursors of SNe Ia has been discussed for more than 45 years, starting from the papers of Tutukov & Yungelson (1979b); Webbink (1979); Tutukov & Yungelson (1981); Iben & Tutukov (1984); Webbink (1984). The current status of the problem is considered, for example, in the recent reviews by Hillebrandt et al. (2013); Maoz et al. (2014); Postnov & Yungelson (2014); Ruiz-Lapuente (2014).

There are two main competing hypothetical scenarios of the evolution of close binaries to SNe Ia: (a) the ‘single-degenerate’ one (SD), implying the explosion of a CO WD

that accumulated matter from a non-degenerate donor and (b) the ‘double-degenerate’ scenario (DD), in which SN Ia is a result of the merger of a pair of WD. Other scenarios, such as a merger of WD with the core of a red giant (core-degenerate one in modern terms) (Sparks & Stecher 1974; Ikov & Soker 2012) or direct collisions of WD (Raskin et al. 2009; Rosswog et al. 2009b) are usually considered to be less important. We do not consider SNe Ia induced by tidal interactions of WDs with black holes (Rosswog et al. 2009a) and ‘resonant’ ones (McKernan & Ford 2016), as well as the possible enhancement of SNe Ia rate owing to dynamical interactions in stellar clusters (Shara & Hurley 2002).

The topic of the present paper is the double-degenerate scenario. Its main assumption is that the loss of angular momentum via gravitational wave radiation by a close binary with WD components reduces separation of the WD and leads to the Roche lobe overflow (RLOF) by the lower mass one (with the larger radius). Early simple analytical estimates using mass-radius relation (Tutukov & Yungelson 1979b) suggested that for mass-ratio of components $\gtrsim 2/3$, mass-loss by the WD becomes unstable and the latter completely disrupts, presumably on a time scale comparable to the orbital period of the

* E-mail: lev.yungelson@gmail.com

system P_{orb} , forming a disk that gradually settles onto the WD. Components of the binary thus ‘merge’. Later, Nelemans et al. (2001b); Marsh et al. (2004) showed that the stability of mass loss depends also on the efficiency of the tidal interaction in the binary. SPH-calculations taking into account the physical equation of state demonstrated that WD disrupts in $\sim 100P_{\text{orb}}$ and merger occurs in the direct impact regime (e. g., D’Souza et al. 2006; Dan et al. 2009, 2011). While the early versions of the scenario assumed as precursors of SN Ia only pairs of CO WD with $M_1 + M_2 \geq M_{Ch}$ (Tutukov & Yungelson 1979a; Webbink 1979; Tutukov & Yungelson 1981; Webbink 1984; Iben & Tutukov 1984), currently, mergers of sub- M_{Ch} systems with CO accretors and CO, He and hybrid donors¹ are considered too. The evidence for the necessity of consideration of sub- M_{Ch} SNe Ia was summarized by van Kerkwijk et al. (2010).

However, an essential problem that is apparently unresolvable in the foreseeable future is that the disruption of the donor and formation of a quasi-steady configuration are modelled by SPH-methods, with resolution $\sim 10^7$ cm at best, while models of nuclear burning deal with scales down to ~ 1 cm. SPH-computations allow us only to determine whether the necessary condition of detonation – an energy release time-scale $\tau_{3\alpha}$ is shorter than the local dynamical time-scale τ_{dyn} – is fulfilled, while the necessary and sufficient condition for self-sustained detonation is the supersonic speed of flame propagation. If it does not follow immediately from the computations of merger that the latter condition is fulfilled, one has to judge whether detonation is possible, using results of SPH-calculations as an input for mesh-based codes of different degrees of sophistication. The aim is to find whether formation of ‘hot spots’ in the merger products is possible, that is, to calculate the critical sizes of hot regions that ignite and yield propagating detonations. The parameters of hot spots (density, temperature and its gradient, geometry) for He were found by 1-D calculations by Holcomb et al. (2013); Shen & Moore (2014) and for C/O mixture, most recently, by Seitenzahl et al. (2009); Shen & Bildsten (2013)².

The above circumstance makes the real role of the DD-channel in production of SNe Ia uncertain. The aim of the present study is to estimate possible contribution of the DD-scenario to the rate of SNe Ia and dependence of delay-time distribution for SNe Ia on this scenario under an *extreme assumption that all mergers of super- M_{Ch} CO+CO pairs of WD, as well as mergers of CO WD and massive He and hybrid WD result in SNe Ia*.

In § 2 we briefly review the extant results of merger computations and show that they are still inconclusive. For this reason, we compute the total rate of mergers of WD pairs

¹ $M \simeq (0.32 - 0.60)M_{\odot}$ CO WD that descend from helium stars and have mass abundances of He up to almost 90% in the $\simeq(0.20 - 0.01)M_{\odot}$ envelopes; more massive post-He-stars WD have only traces of He in their envelopes.

² Such a method may lead to the smoothing of temperature distribution and distortion of the distribution of chemical species, potentially influencing results of calculations, see, for example, the detailed discussion by Shen & Moore (2014); Katz et al. (2016). Another important factor is sophistication of the nuclear reactions grid.

with He, hybrid- and CO-donors and CO or ONe accretors for different parameters of population synthesis, aiming to estimate the upper limit of contribution of mergers to SNe Ia rate and, particularly, of different pairs to the latter. In § 3 we present the assumptions we use, in § 4 our results are presented, followed by Discussion in § 5 and Conclusions in § 6. Some additional information is provided in the Appendix.

2 MERGER COMPUTATIONS

The merger of WD may proceed through several stages: (i) disruption of the less-massive WD and dynamical accretion; (ii) relaxation of the resulting configuration to the quasi-steady state; (iii) evolution of the merger product to a SN or an accretion induced collapse (AIC).

Merger products have a similar structure (Guerrero et al. 2004): a cold virtually isothermal core, a pressure-supported envelope, a Keplerian disc, and a tidal tail. If explosion does not happen during dynamical stage of merger, He or C/O-mixture may explode in the envelope which is the hottest part of the object. Detonation of He in the envelope may lead to the detonation of carbon at the periphery of accretor (‘edge-lit detonation’) or in its central region which is compressed by converging shocks (‘double-detonation’). The explosion of a CO WD results in its complete disruption. While the mayor fraction of the accretor mass burns to radioactive Ni, which determines optical luminosity and spectrum of the SN Ia, the donor burns to intermediate mass elements which are responsible for observational manifestations of SN Ia at maximum brightness (Shigeyama et al. 1992; Sim et al. 2010). Thus, the main role of the donor explosion (or of its remnants after disruption) is to trigger the detonation of the accretor (Rosswoog et al. 2009b).

Sub- M_{Ch} ‘double-degenerate’ scenario is to a significant extent related to the also still hypothetical ‘double-detonation’ scenario with a He-rich donor, either degenerate or non-degenerate, e. g., Livne & Glasner (1991); Shen & Bildsten (2014). Sim et al. (2010), based on a series of 1-D calculations of pure detonations of CO WD with post-processing nucleosynthesis and radiation transfer, concluded that sub- M_{Ch} explosions are a viable model for SNe Ia for *any* evolutionary scenario leading to explosions in which the optical display is dominated by the material produced in the detonation of the primary WD.

Systematic studies of mergers of WD pairs with He WD or CO/He hybrid WD donors and CO WD accretors with mass from $0.4 M_{\odot}$ to $1.2 M_{\odot}$ were performed by Guillochon et al. (2010) and Dan et al. (2012, 2014), using grid-based and SPH-codes, respectively. They found that for He/hybrid+CO pairs of WD the condition $\tau_{3\alpha} \leq \tau_{\text{dyn}}$ is fulfilled prior to merger or at the surface contact provided $M_{CO} \leq 1.1 M_{\odot}$ and mass of He-rich donor $\gtrsim 0.4 M_{\odot}$. In some cases detonation is due to instabilities in the accretion stream. It remains unclear, however, whether these surface detonations may initiate detonation in the core. For CO+CO WD pairs dynamical burning conditions were met for $(M_1 + M_2) \geq 2.1 M_{\odot}$ only.

Pakmor et al. (2010, 2012) studied ‘violent’ (see below) mergers of several pairs of equal and almost equal mass CO WD ($M_1 = 0.9 M_{\odot}$) in which they *assumed*, based on com-

putations of [Seitenzahl et al. \(2009\)](#) that detonation occurs if, during compression and heating of the matter encountering the accretor, the threshold $T \gtrsim 2.5 \times 10^9$ K at the density of about $2 \times 10^6 \text{ g cm}^{-3}$ is reached. As a critical mass ratio for detonation, [Pakmor et al.](#) inferred $M_2/M_1 = 0.8$. Having in mind that the traces of He ($10^{-3} - 10^{-2}$) M_\odot should be present at the surface of all CO WD and that He is ignited more readily than carbon and, thus, may facilitate nuclear ignition during the merger ([Guillochon et al. 2010](#)), and based on the computation of merger of $1.1 M_\odot$ and $0.9 M_\odot$ WDs with $0.01 M_\odot$ He-envelopes, [Pakmor et al. \(2013a\)](#) speculated that He-ignited (CO+CO) WD and (CO+He) WD mergers may present a unified model for normal and rapidly declining SNe Ia. The model does not explain SNe Ia with strongly mixed ejecta (SN 2002cx type ones).

[Ruiter et al. \(2013\)](#) used the relationship between accretor mass and M_{bol} in maximum for detonating sub- M_{Ch} mass CO WD to construct the brightness distribution expected for violent mergers of pairs of CO WD by population synthesis. Under certain assumptions, the shape of brightness amplitude distribution matches the observations well. However, the model needs further elaboration in respect of nuclear display and spectral features. At the moment, it is worth to mention that the model encounters serious difficulties in reproducing spectrophotometric features of SNe Ia because of asymmetries in the distribution of ejecta ([Bulla et al. 2016](#)).

[Dan et al. \(2015\)](#) analysed possibility of post-merger explosions for some previously found configurations, using them as an input for the grid-based 2-D hydrodynamical calculations with account of rotation by the code FLASH ([Fryxell et al. 2000](#); [Dubey et al. 2009](#)). It was found that *immediately* after completion of merger detonation does not occur in either He+CO or CO+CO pairs, because of too low a density of hot regions (envelopes). To the similar conclusion for CO+CO pairs came [Zhu et al. \(2013\)](#); [Tanikawa et al. \(2015\)](#); [Sato et al. \(2015\)](#). However, it was suggested that an insufficient resolution in most computations, $\lesssim 500k$ ($k = 1024$ particles per M_\odot), may be the reason for this ([Sato et al. 2016](#)). In test computations with resolution up to $\approx 2000k$ in which also $^{12}\text{C} + ^{12}\text{C}$ reaction was taken into account, detonation conditions of [Seitenzahl et al. \(2009\)](#), were met by pairs of WD with $M_1 \gtrsim 0.8 M_\odot$ and

$$M_2/M_1 \gtrsim 0.8 (M_1/M_\odot)^{-0.84}. \quad (1)$$

One may expect that a further increase of resolution, will allow to resolve smaller hot regions. [Sato et al. \(2016\)](#) also noted that the study of possible mergers at contact for He+CO pairs needs a higher resolution, since the occurrence of helium detonation depends strongly on the mass of the helium layer. This may affect 'unified' model of [Pakmor et al. \(2013b\)](#).

[Dan et al. \(2015\)](#) found that the criteria of spontaneous detonation discovered by [Holcomb et al.](#), [Holcomb et al. \(2013\)](#), [Shen & Moore \(2014\)](#), [Seitenzahl et al. \(2009\)](#) may be met during evolution of merger products in their most dense and hot regions. However, because of above-mentioned discontinuity in resolution of SPH and mesh-based computations, hot spots were located 'manually', assuming that the merger products evolved to conditions necessary for deto-

nations. It was found that He-detonation, may lead or not lead to the detonation in the centre, As well, it was found that the initial perturbation may not initiate detonation in the envelope, but converging shocks may cause detonation in the core. Some of post-merger configurations do not lead to SN Ia³.

[Raskin et al. \(2012\)](#), who also computed the merger of WDs by SPH, have shown that in the models of merger of CO WD with He-envelopes ($M_{1,2} = (0.64 - 1.06) M_\odot$, $M_{He} = (0.013 - 0.015) M_\odot$), He detonates in the merger process, but the released energy is not sufficient for initiation of detonation in the core of the merger product. In the continuation of this study, [Moll et al. \(2013\)](#), have analysed possibility of detonation using grid-based code with a higher resolution and showed that secondary detonation is possible, if massive ($M_{1,2} \gtrsim 1.06 M_\odot$) WD merge. But we note that, like in the studies of [Pakmor et al.](#), these computations rely on artificial ignition of detonation.

The long-term post-merger evolution of the merger product of CO WDs which avoided detonation at the merger itself was simulated by [Shen et al. \(2012\)](#); [Schwab et al. \(2016\)](#) using α -viscosity prescription. [Schwab et al. \(2012\)](#) performed a similar study for a He+CO WD merger. It was found that merger products evolve on the viscous time scale towards spherical configurations. A hot, slowly rotating, and radially extended envelope forms. Certain amount of mass may be lost by the stellar wind. At the end of this stage, owing to dynamical and viscous heating, the temperature at the base of the envelope may become high enough for off-centre burning. In the case of He/CO mergers, it is possible that He-detonation ensues and a SN Ia explodes. As argued by [Schwab et al. \(2016\)](#) on the basis of 1-D computations, in the case of CO WDs, if the mass of the object remains below $1.35 M_\odot$, inward propagation of the burning leads to formation of a massive ONe WD. In merger remnants with higher mass, neon ignites off-centre. It is expected that a silicon WD forms. If the mass remains super- M_{Ch} , further nuclear evolution will result in formation of an iron core and collapse, producing a neutron star. The optical manifestation of an accompanying supernova is uncertain. In fact, the study of [Schwab et al.](#) questions the role of mergers of CO WD with mass below $\approx 2 M_\odot$ as progenitors of SNe Ia in the DD-scenario.

[Ji et al. \(2013\)](#) have shown (in 2-D) that the merger of a pair of $(0.6+0.6) M_\odot$ CO WDs produces a rapidly-rotating WD surrounded by a hot corona and a thick, differentially-rotating disk, which is strongly susceptible to the magnetorotational instability. Instability leads to the rapid growth of the initially dynamically weak magnetic field in the disk, spin-down of the 'new-born' WD, and to the central ignition of the latter. However, as the outcome of ignition depends on the temperature profile ([Seitenzahl et al. 2009](#)), this simulation also does not definitely tell whether SN Ia explodes. Consideration of magnetic field evolution of merger product of $M_1 + M_2 < M_{Ch}$ WD ([Zhu et al. 2015](#)) has shown

³ A caveat should be inserted that results of [Dan et al.](#) may be influenced by assumption that their initial models of CO WD with mass $0.45 M_\odot$ to $0.6 M_\odot$ have a $0.1 M_\odot$ helium mantle; such an abundance may be an overestimate ([Iben & Tutukov 1985](#); [Chen & Han 2002](#)).

that exponential amplification of the field strengths occurs. [Zhu et al.](#) speculated that magnetic field provides a mechanism for angular momentum transfer and additional heating, facilitating carbon fusion.

However it was pointed out earlier ([Piersanti et al. 2003b](#)) that, if a Keplerian disk forms out of the disrupted component and persists, as a result of the spin-up of rotation of the WD by accretion, instabilities associated with rotation, deformation of the WD, and angular momentum loss by a distorted configuration via gravitational waves, accretion rate onto WD that is initially $\sim 10^{-5} M_{\odot}/\text{yr}$ decreases to $4 \times 10^{-7} M_{\odot}/\text{yr}$ and close-to-centre ignition of carbon becomes possible. This self-regulated accretion mechanism is applicable for pairs with total mass (1.4–1.5) M_{\odot} at the onset of carbon ignition; its timescale is $\sim 10^6$ yr.

[Kashyap et al. \(2015\)](#) performed a post-merger evolution simulation for a (1.1+1.0) M_{\odot} CO+CO WD system and found that a spiral-mode instability developed in the accretion disk on the dynamical time-scale and forced hot disk material to accrete onto the core of the remnant. This process drives a thermonuclear outburst leading to SN Ia without the need for artificial ignition. This mechanism works on the time scale which is two-three orders of magnitude shorter than the magneto-rotational instability suggested by [Ji et al. \(2013\)](#). Thus, a self-ignited detonation may be possible in post-merger stage at least for the most massive objects. However, follow-up modelling of light-curve and spectrum of the system ([van Rossum et al. 2016](#)) led to the suggestion that a better agreement with observables of normal SNe Ia will require lower masses of components, but whether similar mechanism will be effective for these systems remains an open question. Nevertheless, as noted by [Kashyap et al. \(2015\)](#), a wide range of He+CO WD mergers may ignite unstable helium burning via the spiral-wave mechanism. An attractive feature of the above-described mechanism is that detonation occurs within ~ 100 s after merger and ejectum will not interact with any significant amount of the matter lost from the disk and produce additional radiation in the early light-curve which may be misinterpreted in favour of the presence of a non-compact progenitor ([Levanon et al. 2015](#)).

Note that at difference to the simulations of SNe Ia by some other authors, [Dan et al. \(2012, 2014\)](#); [Moll et al. \(2014\)](#); [Sato et al. \(2015\)](#); [Sato et al. \(2016\)](#) took as initial models for exploration of possibility of SN Ia the ones obtained by computations of WD merger, instead of taking an equilibrium hydrostatic model or a model, obtained by the accretion of He onto CO WD. It is assumed initially that WDs rotate synchronously ([Fuller & Lai 2012](#); [Burkart et al. 2013](#)). In the case of non-synchronous rotation, disruption of the lower-mass WD occurs on shorter time-scale ($\sim 10 P_{\text{orb}}$) and is more ‘violent’ ([Dan et al. 2011](#)). In the case of non-synchronous initial rotation, nuclear burning starts at larger densities and it is more probable that SN Ia occurs (e.g., [Pakmor et al. \(2012, 2013a\)](#)). As noted by [Dan et al. \(2014\)](#), it is likely that in the latter case detonation happens in the centre of the merger product, while in the former case, at the core surface. As a result, there may be differences in the amount of unburned matter, ejectum velocity and ejectum asymmetry. However, the issue of initial conditions still remains controversial.

A special case is the still badly explored mergers in-

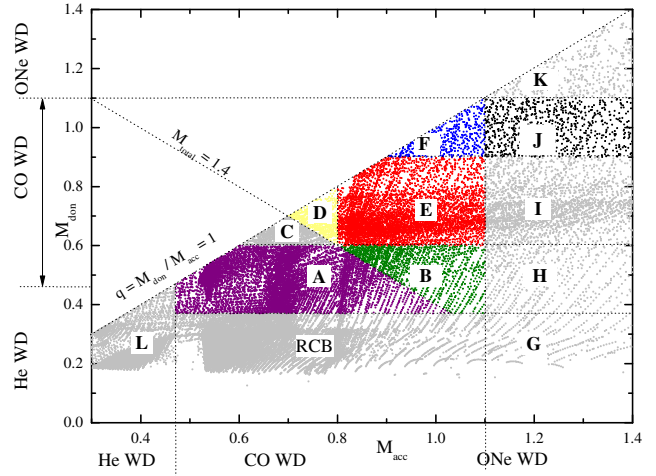


Figure 1. Breakdown of the $M_{\text{acc}} - M_{\text{don}}$ diagram into subregions. See the text for a detailed description. The density of dots in the particular regions of the diagram is proportional to the number of pairs of WDs that merge over 10 Gyr after an instantaneous star-formation burst for simulation with $Z=0.02$, $\alpha_{\text{ce}}\lambda=2$, and tidal effects taken into account.

volving ONe WD. If the disrupted dwarf is He-rich, one may expect He detonation followed by core collapse, if the remaining mass exceeds M_{Ch} . Such an SN would be classified as a SN Ib (e. g., [Kitaura et al. 2006](#)). Whether He-detonation can in this case robustly trigger close-to-centre detonation remains an unsolved problem ([Shen & Bildsten 2014](#)). [Marquardt et al. \(2015\)](#) speculated that thermonuclear runaway in the core of ONe WD *may* be triggered externally and explored such a detonation. They concluded that observationally such explosions will be quite similar to SNe Ia produced by detonations of similar mass CO WD.

To summarize, a clear apprehension of the nature of progenitors of SNe Ia in the DD-scenario and processes occurring during the merger of WDs and in the post-merger stage is currently lacking.

3 THE MODEL

For clarity, we reproduce in Fig. 1 slightly modified $M_{\text{acc}} - M_{\text{don}}$ diagram for merging WDs ([Dan et al. 2014](#)) which we split into 13 subregions (zones) where the pairs of WD of different mass and chemical composition merge and different outcomes of merger are possible, including SNe Ia. We set the lower mass limit for possibly detonating He WD at $0.37 M_{\odot}$; above this limit detonations in the stream and at the contact are possible ([Dan et al. 2011, 2012](#)), though, according to [Holcomb et al. \(2013\)](#), virialised He WD even with $M_{\text{He}} \geq 0.24 M_{\odot}$ may detonate. Despite the fact that maximum mass of degenerate helium cores of stars slightly decreases with stellar mass ([Sweigart & Gross 1978](#)), we use the ‘canonical’ value of $0.47 M_{\odot}$ as the lower limit for the masses of CO WD produced by AGB-stars. We consider also ‘hybrid’ WD. Like for He WD, the lower boundary of the mass range of exploding hybrid WD is set to $0.37 M_{\odot}$.

Since we aim to evaluate the upper limit of SNe Ia rate

provided by merging of WDs, we consider as SNe Ia all mergers of CO and He or hybrid WD in which at least one detonation event is expected, though, as it is shown in the previous section, this issue is still open. It is unsolved, whether all such events will be identified with SNe Ia.

We expect the following events in the zones marked in Fig. 1.

A. Merger of He or hybrid WD with a CO WD resulting in He detonation in the envelope and possible subsequent detonation of carbon in the core.

B. Merger of He or hybrid WD and CO WD resulting in detonation of both WD.

C. Merger of CO WDs with $M_1 + M_2 < M_{Ch}$ with the formation of a massive single WD.

D. Merger of comparable mass CO WDs with an explosion in the post-merger process.

E. Merger of massive CO WDs leading to SN Ia in the post-merger stage.

F. Merger of similar mass CO WDs with an SN Ia explosion in the merger process.

G. Merger of a massive He WD or a hybrid WD with ONe WD with subsequent (AIC).

H. Merger of an ONe WD with a hybrid WD with subsequent AIC.

I. Merger of a CO and an ONe WD with subsequent AIC of the ONe core.

J. Violent merger of an ONe WD with a CO WD resulting in C detonation with subsequent detonation of the ONe WD (Marquardt et al. 2015). Dan et al. (2012) have shown that C-transferring systems do not detonate at contact.

K. Merger of ONe WDs. Thermonuclear explosion is possible, if the envelopes contain He. Such an event may be classified rather as a SN Ib than a weak SN Ia.

L. Merger of low-mass He or hybrid WD leading to formation of helium subdwarfs. No SN Ia are produced.

RCB. Merger of He and CO WDs in which the necessary conditions for He detonation are not met. Hypothetically, such mergers may lead to the formation of R CrB stars (Webbink 1984; Iben et al. 1996); evolution of the latter is defined by competition of core growth due to He-shell burning and mass loss by stellar wind. The growth of the core mass to M_{Ch} and explosion are not very likely, but if they happen, the event would probably be observed as a peculiar SN Ib.

In assigning SN Ia status to the outcome of merger, we used, primarily, numerical results and qualitative considerations presented in Dan et al. (2014, 2015), as well as data from literature discussed in § 2. Accordingly, we consider as SNe Ia results of mergers occurring in the zones **A**, **B**, **D**, **E**, **F**, and **J**, although we clearly recognize that all of them are still hypothetical. We note the following. If detonation of He in the pairs merging in the zones **A** and **B** does not initiate CO-core detonation, He explosions may be still identified with subluminous SNe Ia (Shen et al. 2010; Waldman et al. 2011). In zone **C** mergers do not result in SNe Ia according to Eq. (1); furthermore, M_{acc} should exceed about $0.8 M_{\odot}$. In zone **D** undisrupted CO WD accumulates M_{Ch} via self-regulating accretion in $\sim 10^6$ yr (Piersanti et al. 2003a). To mergers in zones **E** and **F** the status of SN Ia is assigned according to results of Sato et al. (2015) and Moll et al. (2014); Kashyap et al. (2015), respectively. As concerns pos-

sible explosions of ONe WD, Marquardt et al. (2015) have shown that the detonations of these objects are possible, given that there is an external trigger. Appropriate computations are absent, but it is clear that the ‘trigger’ dwarf has to be massive or such events may not happen at all. Thus, our limiting $M_{don} = 0.9 M_{\odot}$ may be too optimistic. Note, however, that the contribution of zone **J** to the rate of SNe Ia in the case $\alpha_{ce}\lambda=2$, which we consider as giving the best agreement with observations, does not exceed 10 per cent (see § 4).

3.1 Population synthesis

For the modelling of the population of merging WDs, we applied the code BSE (Hurley et al. 2000; Hurley et al. 2002; Kiel et al. 2008). The advantage of BSE is that it is based on a homogeneous system of evolutionary tracks for single stars with metallicity from $Z = 0.0001$ to 0.02 (Pols et al. 1998), which was used to construct analytical approximations describing stellar evolution. The shortcoming of BSE is that the evolution of binaries is treated on the base of assumptions originating from the work of other authors or (educated) guesses for never calculated evolutionary transitions.

Our results are based on the modelling of 10^7 initial systems and for each set of initial parameters represent one realization of the model. Hence, they are subject to Poisson noise.

Taking into account recent suggestions on the dependence of the binarity rate on the mass of stars, we approximated this rate as (van Haaften et al. 2013)

$$f_b = 0.50 + 0.25 \log(M_1/M_{\odot}). \quad (2)$$

Common envelopes. The problem of common envelopes (CE) is the most acute one in the theory of evolution of close binaries; see Ivanova et al. (2013) for a recent detailed discussion. In the context of the problem we address in the present study, CE form when accretor is not able to swallow all the matter supplied by the donor or the system is subject to the Darwin instability.

There is no unanimous opinion on the form of the equation describing the evolution of stars in the CE. We apply an equation suggested by Tout et al. (1997), included in BSE as an option, because in our opinion, it better accounts the expenditure of energy on the expulsion of the CE than the ‘standard’ (Webbink 1984; de Kool 1990) equation, if both components have clear-cut cores and envelopes. However, test runs with ‘standard’ equation show that the difference in the rates of SNe Ia does not exceed 10 per cent. The basic problem of both formulations of the CE equation is that its solution for the ratio of the initial and final separations of the components, upon which it is decided whether the components merged, depends on the product of two parameters – $\alpha_{ce}\lambda$. The ‘common envelope efficiency’ α_{ce} describes the efficiency with which the spiralling-in cores of components transfer orbital energy to the envelope and disperse the latter; it is expressed in fractions of the orbital energy of the system. Parameter λ characterizes the binding energy of the donor envelope.

A problem related to the outcome of the CE was noted by Kashi & Soker (2011): while CE equation(s) may formally imply that the system remains detached at the end of

the CE stage, in fact some matter of the envelope may not reach escape velocity and remains bound to the system and form a circumbinary disc. Angular momentum loss owing to interaction with the disk may result in further reduction of the binary separation and the merger of components. This may influence, among other populations, SNe Ia, but this problem remains unsolved. On the other hand, the influence of this phenomenon is partially compensated by uncertainty in the treatment of CEs in general.

Both parameters describing the CE are still highly uncertain. For α_{ce} , the most important issue is whether there are other sources than orbital energy for expulsion of CEs, that is, whether $\alpha_{ce} > 1$ is possible. In fact, α_{ce} is a specific parameter of any CE. The use of it is forced, because for a given system with components at different evolutionary stages and particular combination of M_1 , M_2 , a , the outcome of the CE may be found only by 3D hydrodynamical calculations, which still have insufficient resolution or do not account for all physical processes occurring in CEs on different time scales (Ohlmann et al. 2016). It is evident that λ should continuously vary in the course of stellar evolution; position of the core-envelope boundary remains uncertain – the value of λ may be uncertain by a factor of 10 depending on the definition of the core-envelope boundary (Tauris & Dewi 2001). Regarding ‘observational’ estimates, one should bear in mind severe selection effects which may restrict the observed population to fractions of per cent of the intrinsic one, resulting in poor statistics (see e. g. Camacho et al. 2014).

Nevertheless, we consider it justified to use as a constant parameter the value(s) of α_{ce} found for sufficiently representative samples of close binaries that evolved through the CE stage or were derived by the study of particular binaries. However, it appears, for instance, that for low-mass systems – post-CE binaries (PCEB) with $M_2 \lesssim 0.8 M_\odot$ from SDSS – the estimates of α_{ce} range (within error bars) between 0.02 and 10 (Zorotovic et al. 2010). Within this range, for the systems with AGB progenitors, α_{ce} values cluster below 0.2, while for those with FGB progenitors almost all α_{ce} values are $\gtrsim 0.2$. Thus, the quite common claim that $\alpha_{ce} \approx 0.2–0.3$ seems to be not well justified. The population of well-studied binary WDs, after accounting for observational selection, is rather well reproduced with $\alpha_{ce}\lambda=2$ (Nelemans et al. 2001a; Toonen et al. 2012). Therefore, we performed simulations for $\alpha_{ce}\lambda$ in the range from 0.25 to 2, but consider the version with $\alpha_{ce}\lambda=2$ as the main one; see § 4. In a similar way, in their studies of SNe Ia, Mennekens et al. (2010) parametrized CEs by $\alpha_{ce}\lambda=1$, while Toonen et al. (2012, 2014) used $\alpha_{ce}\lambda=2$.

Stability of mass-exchange. An under-researched topic in binary star evolution is the stability of mass loss by stars with deep convective envelopes and He-stars.

For hydrogen-rich stars we kept the stability criteria accepted in BSE. For helium stars – the remnants of components of binaries with mass $\gtrsim (2.0–2.5) M_\odot$, which experienced RLOF in the hydrogen-shell burning stage (case B of mass-exchange), stability criteria were modified. Paczyński (1971); Iben & Tutukov (1985) have shown that He stars with masses below $(0.8–0.9) M_\odot$ do not expand after He exhaustion in their cores and evolve straight into hybrid WD. More massive He stars expand in the He-shell-burning stage; the extent of the expansion depends on the mass of the star and RLOF may restart if the components are close enough.

Based on trial computations of semidetached binaries with He donors (D. Kolesnikov et al., *in prep.*) we consider mass loss unstable if stellar radius becomes $\geq 5 R_\odot$ and $q \geq 0.78$. If R_{He} remains below $5 R_\odot$, the critical $q = 3.5$.

Angular momentum loss via gravitational waves radiation may bring low-mass He stars into contact with WD prior to He exhaustion in their cores. In the systems where conditions for stable mass exchange are fulfilled, initially, $\dot{M} \sim 10^{-8} M_\odot/\text{yr}$ (Savonije et al. 1986; Iben & Tutukov 1991; Yungelson 2008). At these \dot{M} , surface detonation of He is possible (Taam 1980; Nomoto 1982). We exclude such systems from further consideration, because they are not of interest in the present study. Such binaries are suggested to be progenitors of double-detonation SN Ia, but the real efficiency of this scenario is under debate (Piersanti et al. 2014, 2015; Brooks et al. 2015).

For WDs, the stability of mass exchange depends on the mass ratio of components and efficiency of spin/orbit coupling (Nelemans et al. 2001b; Marsh et al. 2004). As well, it is possible that tidal interaction allows stable mass transfer, but the rate of the latter is super-Eddington and a CE may form. We considered mass transfer between WDs as stable, irrespective of the efficiency of spin/orbit coupling, if its rate remains sub-Eddington and M_{don} (in solar units) satisfies the following approximation based on fig. 1 of Dan et al. (2011):

$$M_{\text{don}} \leq \begin{cases} 0.2286 M_{\text{acc}}, & \text{if } M_{\text{acc}} \leq 0.875; \\ 0.133 M_{\text{acc}} + 0.0833, & \text{if } 0.875 < M_{\text{acc}} \leq 1.1; \\ -0.033 M_{\text{acc}} + 0.2667, & \text{if } 1.1 < M_{\text{acc}} \leq 1.44. \end{cases} \quad (3)$$

Tidal effects. Tidal effects are significant predominantly for giant stars. The main evolutionary consequence of tides is earlier RLOF, if the tides are taken into account. For instance, RLOF in RG-stage instead of AGB-stage may occur and a He or hybrid WD to form instead of a CO WD. On the other hand, for later RLOF, formation of a CE and merger of components inside them is more probable. There is no consensus on the account of tides in binary population synthesis (BPS); see comparison of assumptions in table 1 of Toonen et al. (2014). For instance, they were not taken into account in the latest simulations of Claeys et al. (2014). We used the algorithm for the account of circularisation of the orbits and synchronization of rotation as it is incorporated in BSE: according to Zahn (1975) for stars with radiative envelopes and according to Hut (1981) for stars with convective envelopes.

We implemented in the code modifications to the algorithm of computation of mass transfer rate that make it more stable (Claeys et al. 2014, Eq. (11)).

Star-formation rate. For the estimate of SNe Ia rate in the Galaxy, we accepted that the star-formation rate (*SFR*) in the bulge and thin Galactic disk can be described by a function combining exponentially declining and slow constant components (Yu & Jeffery 2010):

$$SFR(t) = 11 \exp(-(t-t_0)/\tau) + 0.12(t-t_0) M_\odot/\text{yr} \text{ for } t > t_0. \quad (4)$$

Here, time t is in Gyr, $\tau=9$ Gyr, $t_0=4$ Gyr, Galactic age is 14 Gyr. We neglect halo and thick Galactic disk stars with total mass of only several per cent of the mass of the

bulge and thin disk. In the bulge and thin disk $SFR(t) = 0$ at $t \leq t_0$. Current Galactic $SFR=4.82 M_{\odot}/\text{yr}$, well within the range of modern estimates – from ~ 1 to $\sim 10 M_{\odot}/\text{yr}$ (Gilmore 2001). The total mass of the bulge and the disk is then $7.2 \times 10^{10} M_{\odot}$, close to the estimate of Klypin et al. (2002) – $7.0 \times 10^{10} M_{\odot}$.

We neglect in the models stellar winds of He stars, because extrapolation of the rates for WR stars or Reimers-type winds assumed in BSE is not justified and, even then, winds are hardly evolutionary meaningful, because of extremely short lifetimes of He stars.

4 RESULTS

4.1 Scenarii for the formation of merging WDs

Population synthesis calculations generate hundreds of evolutionary scenarios. However, the dominant fraction of merging WDs of interest usually form, via only a few channels, differing mainly by the stage in which initially more massive component overflows its Roche lobe. Despite these scenarii were analysed many times, starting from semi-analytical studies by Tutukov & Yungelson (1981); Iben & Tutukov (1984); Webbink (1984) and, most recently, by for example Ruiter et al. (2009); Mennekens et al. (2010); Toonen et al. (2014); Claeys et al. (2014), they still deserve attention.

The fraction of stars evolving via certain channels depends, mainly, on the accepted criteria of the stability of mass loss, the treatment of CE stage(s), the mass and momentum loss from the system, treatment of accretion onto compact stars and criteria according to which the stars are considered as ‘merged’. For instance, compare the simulations of Mennekens et al. (2010) and Toonen et al. (2012) which differ in the assumed radii of stellar remnants and $\alpha_{ce}\lambda$ values – 1 in Mennekens et al. and 2 in Toonen et al.. In the first study, 80 per cent of CO WD and CO cores of donors merge in the CE, while in the second one only 45 per cent do.

Eight main scenarii, which in our simulations result in the formation of not less than about 90 per cent of all merging pairs of WDs, considered as possible precursors of SN Ia are shown in Table 1. The table corresponds to $Z=0.02$, $\alpha_{ce}\lambda=2$ and tides are taken into account. We apply with slight modification the notation accepted in BSE and widely used in the literature: MS, main-sequence star, HG, Hertzsprung gap star, GB, first giant-branch star, CHeB, a star with central He burning, EAGB and TPAGB, early and thermally-pulsating AGB stars, respectively, HeMS, helium-burning remnant of a star, HeWD, COWD, ONeWD, helium, carbon-oxygen and oxygen-neon white dwarfs, respectively. We consider He-shell-burning ‘helium Hertzsprung-gap’ (HeHG in BSE) stars and ‘helium-giants’ (HeG in BSE) as similar objects with CO-cores and helium-burning shells, because they differ only in the extent of expansion of He envelopes. They are identified in Table 1 and in the text as ‘COHe’. For the pairs of WD produced by a certain scenario, we indicate at pre-merger stage the most common combination of components: for instance, scenario 1 is marked as forming a CO WD+CO WD pair, while in fact, about 25 per cent of pairs contain ONe components, owing to a ‘change

of the roles’ during RLOF when initially less-massive secondaries accumulate large mass; we do not consider pairs with ONe WD for computation of SNe Ia rates etc. In Appendix A, in Figs. A1 – A8, we show for these scenarios positions of initial systems in $M_{1,i} - M_{2,i}$, $M_{1,i} - a_i$ and pre-merger $M_{\text{acc}} - M_{\text{don}}$ diagrams. The plots are for the $\alpha_{ce}\lambda=2$ case in which the mergers of WD occur most efficiently (see below).

In scenarii 1 to 4, the first CO WD forms via stable RLOF starting in the Hertzsprung gap or in the first RG-branch (case B of mass exchange). This results in the formation of a He star. As already mentioned, the latter may evolve straight into a CO WD, if their mass is $\lesssim (0.8 - 0.9) M_{\odot}$ or refill Roche lobe and lose some mass (in small-separation systems) for a short time when the star expands on the thermal time scale in the helium-shell burning stage. Because the first RLOF is stable, the secondaries typically accumulate mass larger than $\approx 2 M_{\odot}$ and after mass loss become He-stars. He WD appear only in the side branch of scenario 2 after the CE, if $M_2 \lesssim 2.25 M_{\odot}$. Most merging CO WD+He WD pairs are actually formed by several scenarii that are not among the most prolific ones⁴.

Scenario 1 involves stars more massive than $\simeq 4 M_{\odot}$. Because the masses of components are relatively comparable (Fig. A1) both resulting WDs are quite massive and feed, predominantly zones **E**, **F** and **J**.

Systems with $3 \lesssim M_1/M_{\odot} \lesssim 8$ evolve via scenario 2, but on average these systems have less massive secondaries than in scenario 1. This scenario is to a significant extent similar to scenario 1, but because of the larger span of the initial masses of components it contributes merging pairs of CO WD to virtually all zones of $M_{\text{acc}} - M_{\text{don}}$ plane (Fig. A2). Because the secondaries in some of the initial systems evolving via scenario 2 have initial masses as small as almost $1 M_{\odot}$, certain fraction of former secondaries after mass loss in the CE becomes He WD. However, scenario 2 is not the main channel of He WD formation, most of them form, as mentioned above, via non-common routes. In total, in scenario 2, the fraction of merging He and CO WD pairs feeding zone **A** in Fig. 1 among all merging pairs is 7 per cent for $\alpha_{ce}\lambda=0.25$, 8 per cent for $\alpha_{ce}\lambda=0.5$, 0.3 per cent for $\alpha_{ce}\lambda=1.0$ and 4.5 per cent for $\alpha_{ce}\lambda=2.0$. Most CO and He WD merge in zone **L** where they produce hot subdwarfs or in zone **RCB**, see Fig. 1.

Binaries with $2.5 \lesssim M_1/M_{\odot} \lesssim 8 M_{\odot}$ and less massive secondaries than in the previous scenarios – $M_2 \lesssim 4 M_{\odot}$ – evolve via scenario 3. After the first stable mass exchange these systems become so wide that former initial secondaries overflow Roche lobe only in the EAGB-stage. Their C/O-cores are small, however, and after mass loss in the CE the stars still have relatively massive He envelopes and their evolution is similar to the evolution of He-stars. This scenario con-

⁴ In BSE, as He WD are labelled also descendants of He-burning stars which fill Roche lobes and, because of stable mass loss, have mass reduced below conventional threshold for He-burning of $0.32 M_{\odot}$. In fact, in such stars nuclear burning is frozen almost immediately after RLOF and their interiors may vary from almost pure He to a C/O mixture, depending on the degree of exhaustion of He in the centre at the instant of RLOF. Their entropy is lower than that of He WD – former degenerate cores of red giants (Yungelson 2008). These stars may be donors in systems experiencing single He-detonation or double-detonation.

Table 1. Main evolutionary scenarios leading to formation of merging WD and possible SN Ia. First row: number of the sequence; second row: evolutionary stage preceding the first common envelope episode. Brace by component identifier mean that this star overflows Roche lobe. Absence of brace means that the system is detached. The stages with similar outcome are joined by horizontal braces. ‘CE1’ and ‘CE2’ denote the first and the second common envelope episodes, respectively. For the rest of the notation see the text. Down-arrow symbols indicate that in a particular scenario certain evolutionary stages are absent.

	1	2	3	4
	COWD+HG	COWD+GB	COWD+EAGB	HeMS+GB
1	MS+MS	MS+MS	MS+MS	MS+MS
2	HG+MS		HG+MS	HG+MS
3	{HG+MS	{HG+MS	{HG+MS	{HG+MS
4		{GB+MS	{GB+MS	{GB+MS
5	{GB+MS			↓
6	HeMS+MS	HeMS+MS	HeMS+MS	HeMS+MS
7	COHe+MS	COHe+MS	COHe+MS	HeMS+HG
8	{COHe+MS	{COHe+MS	{COHe+MS	{COHe+GB
9				HeMS+GB
10				HeMS+GB
11	COHe+MS			
12	COWD+MS	COWD+MS	COWD+MS	CE1
13	COWD+HG	COWD+HG	COWD+HG	HeMS+HeMS
14	COWD+HG}	COWD+GB	COWD+GB	COHe+HeMS
15		COWD+CheB	COWD+CheB	
16		COWD+EAGB	COWD+EAGB	COWD+HeMS
17		COWD+GB}	COWD+EAGB}	
18	CE	CE1	CE1	
19				
20	COWD+HeMS	COWD+HeWD	COWD+COHe	COWD+COHe
21	COWD+COHe	COWD+COHe	COWD+COHe	COWD+COHe
22				
23	COWD+ COHe}	COWD+COHe	COWD+COHe}	COWD+COHe}
24		CE2	CE2	CE2
25	↓			
26				
27	COWD+COWD	COWD+HeWD	COWD+COWD	COWD+COWD
28	{COWD+COWD	COWD+HeWD}	COWD+COWD}	{COWD+COWD
29				COWD+ONeWD
30	Merger			
	5	6	7	8
	EAGB+ CheB	TPAGB+ CheB	EAGB+MS	TPAGB+MS
1		MS+MS	MS+MS	MS+MS
2		HG+MS	HG+MS	HG+MS
3			GB+MS	GB+MS
4			CHeB+MS	CHeB+MS
5			EAGB+MS	EAGB+MS
6	GB+MS	HG+HG		
7			{EAGB+MS	TPAGB+MS
8				{TPAGB+MS
9			CE1	CE1
10		GB+HG	COHe+MS	↓
11		GB+GB		↓
12			{COHe+MS	
13				
14		CHeB+GB	COHe+MS	
15		CHeB+CheB	COWD+MS	COWD+MS
16			COWD+HG	COWD+HG
17	EAGB+CheB	EAGB+CheB		
18	{EAGB+CheB	TPAGB+CheB		
19			COWD+HG}	COWD+HG}
20			COWD+GB}	COWD+GB}
21		{TPAGB+CheB		
22				COWD+GB
23				COWD+CheB
24				COWD+EAGB
25				COWD+EAGB}
26				
27		COWD+HeMS	COWD+HeMS	COWD+HeMS
28		COWD+COHe	COWD+COHe	COWD+COHe
29			COWD+COHe}	COWD+COHe
30				
31			COWD+COWD	
32			COWD+COWD}	
33				
34			Merger	

Table 2. Relative number of mergers, possible precursors of SNe Ia, occurring in particular zones of $M_{\text{acc}} - M_{\text{don}}$ diagram over 10 Gyr, for various values of $\alpha_{ce}\lambda$. Column (1), $\alpha_{ce}\lambda$. Column (2), the number of scenario according to Table 1. Column (3), evolutionary stage of the system preceding the first CE. Columns (4) to (9) with headers A to J indicate the relative numbers (in per cent) of WD pairs formed via scenarii listed in column (2) and merging in particular zones of the $M_{\text{acc}} - M_{\text{don}}$ diagram (Fig. 1) over 10 Gyr. Column (10), relative input of a particular scenario into the total rate of WD+WD mergers for a given $\alpha_{ce}\lambda$. Column (11), the ratio of the number of mergers of possible precursors of SN Ia and total number of merging WD pairs for every channel and $\alpha_{ce}\lambda$ value. The absence of data on some scenarios for certain $\alpha_{ce}\lambda$ means that for this $\alpha_{ce}\lambda$ the code does not generate such a scenario at all.

$\alpha_{ce}\lambda$	Sc.	Stage before CE1	Zone of $M_{\text{acc}} - M_{\text{don}}$ diagram						SN Ia	$N_{\text{SN Ia}}/N_{\text{WD2}}$
(1)	(2)	(3)	A	B	D	E	F	J	(10)	(11)
0.25	2	COWD+GB	2.1	-	-	-	-	0.2	2.3	5.60E-03
0.25	3	COWD+EAGB	31.8	12.3	1.3	39.4	1.3	8.1	94.1	2.30E-01
0.25	4	HeMS+GB	-	-	-	-	-	0.6	0.6	1.40E-03
0.25	5	EAGB+CHeB	-	-	-	-	-	0.1	0.1	1.60E-04
0.25		sum	33.8	12.3	1.3	39.4	1.3	8.9	97	2.40E-01
0.5	2	COWD+GB	1.4	0.2	-	1.4	-	2.8	5.8	9.20E-03
0.5	3	COWD+EAGB	50.3	2.9	5.4	24.3	0.7	2.2	85.7	1.30E-01
0.5	4	HeMS+GB	-	-	-	0.5	0.2	0.9	1.6	2.60E-03
0.5	5	EAGB+CHeB	0.8	-	-	-	-	0.2	1	1.60E-03
0.5	6	TPAGB+CHeB	0.2	-	-	-	-	0.02	0.3	4.20E-04
0.5		sum	52.7	3.1	5.4	26.2	0.9	6.3	94.5	1.50E-01
1	1	COWD+HG	-	-	-	-	-	0.2	0.2	2.10E-04
1	2	COWD+GB	5.7	1.3	2.4	10.2	0.1	3.2	23	2.50E-02
1	3	COWD+EAGB	23.4	0.4	2.9	6.8	0.6	2	36.1	4.00E-02
1	4	HeMS+GB	5.1	1.1	3	14.2	0.1	-	23.4	2.60E-02
1	5	EAGB+CHeB	4.5	-	0.01	0.04	0.04	0.3	4.8	5.40E-03
1	6	TPAGB+CHeB	2.4	0.1	0.1	1.4	-	0.03	4	4.40E-03
1		sum	41	2.9	8.5	32.6	0.8	5.7	91.5	1.00E-01
2	1	COWD+HG	-	-	0.2	0.5	0.4	1.1	2.1	5.00E-03
2	2	COWD+GB	9.2	0.5	1.7	5.4	1.2	1.7	19.7	4.60E-02
2	3	COWD+EAGB	2.9	-	0.6	1.3	0.2	0.5	5.5	1.30E-02
2	4	HeMS+GB	16.6	0.3	4.8	7.1	0.004	-	28.8	6.80E-02
2	5	EAGB+CHeB	5.8	-	0.5	0.5	0.02	0.1	7	1.60E-02
2	6	TPAGB+CHeB	2.8	0.04	0.2	0.8	-	0.02	3.9	9.20E-03
2	7	EAGB+MS	2.7	2.2	-	5	-	-	9.9	2.30E-02
2	8	TPAGB+MS	5.6	3.3	0.04	2.1	-	-	10.9	2.60E-02
2		sum	45.6	6.3	7.9	22.9	1.8	3.3	87.8	2.10E-01

tributes to the regions of the $M_{\text{acc}} - M_{\text{don}}$ diagram, where single detonation of He (**A**) or merger of CO WDs with $M_1 + M_2 \geq M_{Ch}$ (**E**, **F**) is possible (Fig. A3).

Scenario 4 is followed by systems with $2 \lesssim M_1/M_\odot \lesssim 7$, with initial separations of components on average smaller than in scenario 3 (Fig. A4). For this reason, prior to the CE, secondaries are still in the RGB-stage of evolution and after mass loss produce He stars. The least massive of He stars evolve straight into hybrid CO WD, while more massive ones expand and the system passes through a second CE (Table 1). If $\alpha_{ce}\lambda \leq 0.5$, scenario 4 produces also some ONeWD+COWD pairs and makes a small contribution to zone **J** (Table 2).

In scenarios 5 – 8, at difference to scenarios 1 – 4, the first RLOF in the system is accompanied by a CE. These systems are wide, the primaries overflow their Roche lobes in EAGB and TPAGB stages of evolution (case C of mass exchange), mass-loss is dynamically unstable. Scenarios 5 and 6 (Figs. A5, A6) are quite similar. Through these scenarios

evolve systems that have similar masses of components. At the time of the first RLOF, companions to mass-losing stars are in the core He-burning stage (Table 1) and the compact cores of both stars appear to be immersed in a ‘double common envelope’. The result of the CE-stage is formation of a COWD+HeMS binary. Merging pairs contain either a CO WD and a hybrid WD or two CO WDs. The outcome of the merger may be single detonation (zone **A**), formation of a massive CO WD (zone **C**) or the merger of (super)- M_{Ch} CO WDs (zones **D** and **E**).

Through scenarios 7 and 8 (Figs. A7, A8) evolve the most wide close binaries with secondaries within quite a large range from $2.5 M_\odot$ to almost $5 M_\odot$. The primaries in these stars overflow Roche lobes in EAGB or TPAGB stage, while their companions still remain MS stars. A CE stage follows. In scenario 7 the donor with small He core first becomes a COHe-star and later – a CO WD. In scenario 7, the separation of components is such that former secondaries overflow their critical lobes in HG or GB stages and turn

into He stars. After exhaustion of He in the cores they evolve into CO WD. Scenario 7 feeds ‘massive’ part of the sub- M_{Ch} zone **B** where both WDs may explode at contact and zone **E**, where (super)- M_{Ch} CO WDs merge. In scenario 8, with the wider initial separation of components, a CO WD is formed straight after the first CE, while the former secondary may, depending on the initial mass and separation, overflow the critical lobe in HG, GB or EAGB stages. In all cases, a CE forms and He stars are formed, which later evolve into CO WDs. Like for scenario 7, scenario 8 feeds massive WD part of zone **A** and zone **E**.

It is worthwhile to note that, while the precursors of most observed binary WD apparently form via two stages of CE (Toonen et al. 2012), most progenitor binaries of merging pairs of WD in our simulations have stable first mass-exchange episode and an unstable (with a CE) second one, as also found by Mennekens et al. (2010); Ruiter et al. (2013). In the simulations of Toonen et al. (2012), the fraction of systems which have only one CE stage is close to 50 per cent.

Above, we presented scenarios dominating in the $\alpha_{ce}\lambda=2$ case. Some scenarios do not realize for all $\alpha_{ce}\lambda$. Furthermore, their relative input varies with $\alpha_{ce}\lambda$. In Table 2 we compare the fractions of systems evolving via scenarios listed in Table 1, depending on $\alpha_{ce}\lambda$ and their input to the particular regions of the $M_{acc} - M_{don}$ diagram. Because of the uncertainty of the value of $\alpha_{ce}\lambda$ we studied the demography of the $M_{acc} - M_{don}$ diagram for $\alpha_{ce}\lambda = 0.25, 0.5, 1.0$ and 2.0.

For $\alpha_{ce}\lambda=0.25$ essentially only scenario 3 can result in the formation of a merging pair of WDs and a SN Ia. Because $\alpha_{ce}\lambda$ is low, this may be understood as a result of the merger of components in CE1 or CE2 in other scenarios. Two branches of evolution can be distinguished, leading, predominantly, to the filling of regions **A** and **E** of the $M_{acc} - M_{don}$ plane. In the first case, a CO WD merges with a hybrid or a He WD, while in the second one, two CO WDs with $M_1 + M_2 \geq M_{Ch}$ merge. The contribution to the two zones is comparable. For $\alpha_{ce}\lambda=0.25$ no systems evolve via scenario 1, that is, mergers of CO and ONe WD do not occur and the ‘triggering’ of explosions of ONe WD simulating SN Ia (Marquardt et al. 2015) is infeasible. For other values of $\alpha_{ce}\lambda$, significance of this scenario is vanishingly small.

Scenario 3 dominates for $\alpha_{ce}\lambda=0.5$ and 1 and feeds predominantly zones **A** and **E** of the $M_{acc} - M_{don}$ diagram. With an increase of $\alpha_{ce}\lambda$ contribution of this scenario to zone **A** first increases, because a larger fraction of low-mass CO WDs avoids merger. However, with a further increase of $\alpha_{ce}\lambda$ over 1, the separation of components after the second CE episode remains so large, that binaries never merge.

For $\alpha_{ce}\lambda=1$, scenarii 2, 4, 5 become significant. In general, as expected, with an increase of $\alpha_{ce}\lambda$, the contribution of systems in which RLOF occurs at later phases, i. e., wider at the zero-age main sequence, increases.

For $\alpha_{ce}\lambda=2$ scenarii 2 and 4 become dominant, and scenarios 5 and 8 provide a significant contribution to zones **A** and **E**. It is important that in all scenarios at least one of the merging WDs is a hybrid one and probably retains some He in the envelope up to the beginning of merger and, in principle, may detonate. Formation of hybrid WD occurs because AGB evolution is typically aborted in a quite early stage, when the CO core is still not well developed and the

post-RLOF star continues its evolution as a star with thick He envelope (COHe in our notation). Similarity between the outcome of cases B and early C of mass exchange was noticed by Iben (1986), but with a caveat that in the case B the stellar remnants are less massive. If RLOF occurred in TPAGB stage, the mass of the nascent WD is also higher than for RLOF in EAGB case, because of the dredge-up event, which occurred in the course of evolution between two stages.

The trends observed in Table 2 are a relatively even (within a factor 1.5) fractional population of regions **A** and **E** of $M_{acc} - M_{don}$ diagram irrespective of $\alpha_{ce}\lambda$ and systematic decrease of the population of regions **F** and **J**, associated with the most massive WDs, with an increase of $\alpha_{ce}\lambda$. Most mergers of WDs occur in zones **A** and **E** (Table 2); that is, as mergers of relatively massive He or hybrid WDs and CO WDs or pairs of CO WDs.

Table 2 clearly shows the influence of the combined parameter $\alpha_{ce}\lambda$ on the merger rate of WDs. In scenarios 1–4, most systems after the first, stable RLOF become so wide that, if the expulsion of the matter from the system in CE is efficient (α_{ce} is high) merger of components is avoided and they form pairs of WDs which are close enough to merge in Hubble time. With an increase of α_{ce} the fraction of merging pairs of WD decreases. Figure A3, as an example, illustrates variation of the initial parameters of systems contributing to scenario 3 for two extreme cases of $\alpha_{ce}\lambda$ and the influence of this parameter on masses and types of merging WD.

We do not present results for the runs with $\alpha_{ce}\lambda > 2$ because such high values of $\alpha_{ce}\lambda$ currently seem unrealistic.

4.2 Delay-time distribution

The fundamental characteristic of SNe Ia is the ‘delay-time distribution’ (DTD); that is, distribution over time-intervals between the formation of a close binary and SN Ia explosion, because every scenario of SN Ia has a typical time scale (Tutukov & Yungelson 1994; Ruiz-Lapuente et al. 1995; Jorgensen et al. 1997; Yungelson & Livio 2000). The empirical DTD is, as a rule, derived from the rate of SNe Ia in the samples of galaxies at large redshifts ($z \sim 1$), but may also be derived for individual galaxies, see Maoz et al. (2014). Theoretically, it is a model of the dependence of the rate of SNe Ia with different precursors on the time elapsed from an instantaneous burst of star-formation that formed a unit of stellar mass. It is evident, that hypothetical SNe Ia associated with short-lived objects, for example, He stars, should have short delays ($\lesssim 1$ Gyr). On the other hand, if particular scenario is associated with potentially long-living objects, like double-degenerates, delays for them may, in principle, overlap with entire lifetime of a galaxy, because most massive WD start to merge in several tens of Myr after a star-formation burst and the upper limit is the Hubble time. Both experimental and theoretical estimates of DTD are overburdened by numerous uncertainties. For empirical estimates, uncertainty may reach an order of magnitude, depending on the sample of SNe Ia under study and possible systematic errors; see Maoz et al. (2014) for a detailed discussion and Fig. 2. The scatter in the theoretical estimates results mainly from the difference in the treatment of evolutionary transformations of binaries in different BPS codes (Toonen et al. 2014).

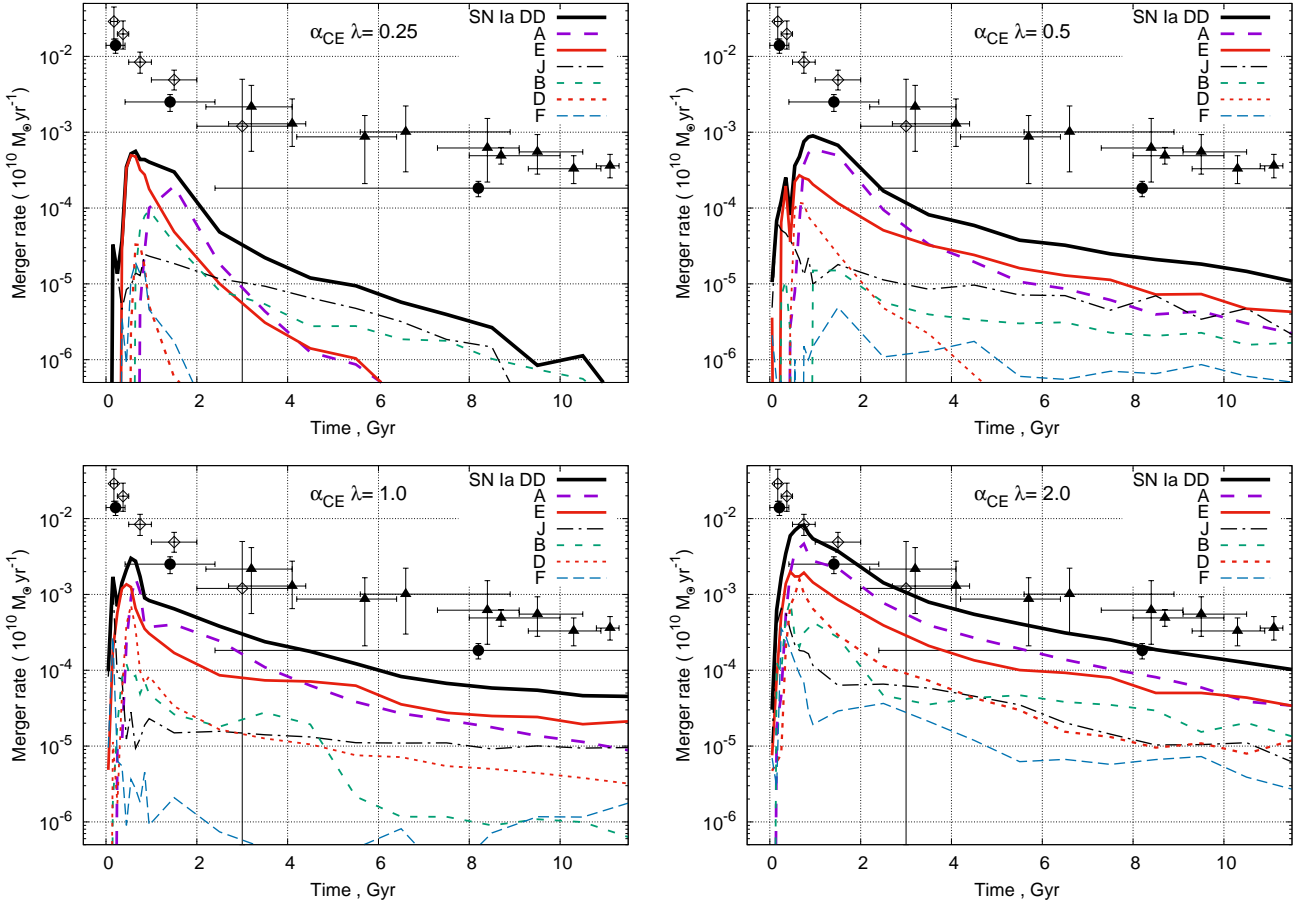


Figure 2. DTD for the model WD+WD mergers potentially producing SNe Ia. Different line styles represent mergers occurring in different zones of the $M_{\text{acc}} - M_{\text{don}}$ diagram, annotated as in Fig. 1. The thick solid line (SN Ia) represents the sum of the models. The models correspond to metal abundance $Z=0.02$. Symbols with error bars: ‘observational’ DTD from Subaru/XMM Survey (Totani et al. 2008), diamonds; galaxy clusters (Maoz et al. 2010), triangles; a sample of field galaxies from the SLOAN II Survey (Maoz et al. 2012), heavy dots.

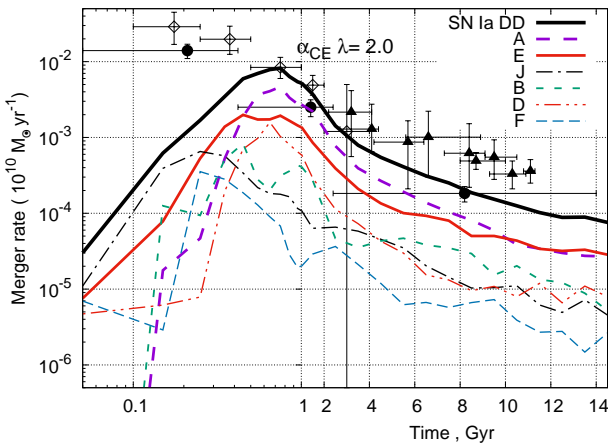


Figure 3. DTD for the model WD+WD mergers potentially producing SNe Ia in the case $\alpha_{ce}\lambda=2$ (similar to the lower right panel of Fig. 2), but showing the DTD for the first 0.05–2 Gyr on a log-scale. Annotation is similar to Fig. 2.

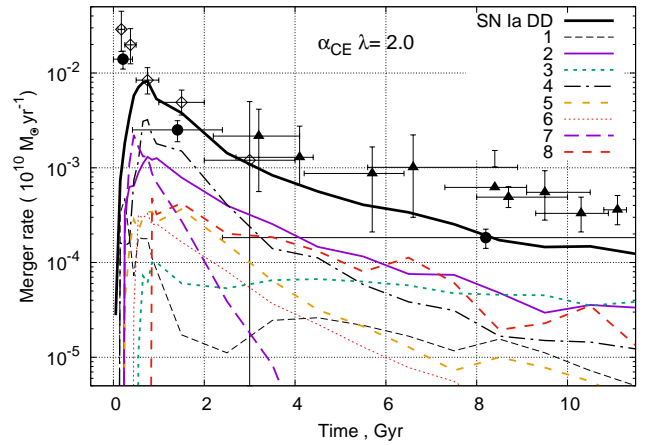


Figure 4. DTD for the WD mergers following scenarios listed in Table 1 for the case $\alpha_{ce}\lambda=2$. Symbols with error bars: ‘observational’ DTD like in Fig. 2.

Table 3. The rate of binary WD mergers occurring at 10 Gyr after an instantaneous star-formation burst in different regions of $M_{\text{acc}} - M_{\text{don}}$ diagram as a function of $\alpha_{ce}\lambda$ (per $10^{10} M_{\odot} \text{yr}^{-1}$). The second column indicates whether SNe Ia are potentially possible. Notation $x(y)$ means $x \times 10^y$.

Zone	DD $M_{\text{accr}} - M_{\text{don}}$	$\alpha_{ce}\lambda$			
		0.25	0.5	1.0	2.0
A	Y	4(-8) \pm 4(-8)	3.7(-6) \pm 5(-7)	1.3(-5) \pm 1(-6)	4.9(-5) \pm 2(-6)
B	Y	7(-7) \pm 3(-7)	2.0(-6) \pm 3(-7)	1.0(-6) \pm 3(-7)	1.8(-5) \pm 1(-6)
C	N	-	6.8(-8) \pm 6(-8)	5.6(-6) \pm 7(-7)	7.8(-6) \pm 9(-7)
D	Y	-	2.3(-8) \pm 3(-8)	4.1(-6) \pm 6(-7)	9.5(-6) \pm 9(-7)
E	Y	-	6.0(-6) \pm 6(-7)	2.2(-5) \pm 1(-6)	4.7(-5) \pm 2(-6)
F	Y	-	7.3(-7) \pm 2(-7)	1.2(-6) \pm 3(-7)	5.6(-6) \pm 7(-7)
G	N	-	6.3(-7) \pm 2(-7)	9.7(-6) \pm 1(-6)	2.2(-5) \pm 1(-6)
H	N	2(-7) \pm 1(-7)	-	-	1.4(-5) \pm 1(-6)
I	N	2.2(-6) \pm 5(-7)	8.5(-6) \pm 7(-7)	1.5(-5) \pm 1(-6)	4.0(-5) \pm 2(-6)
J	Y	3(-7) \pm 2(-7)	4.1(-6) \pm 5(-7)	9.7(-6) \pm 1(-6)	1.1(-5) \pm 1(-6)
K	N	-	4.8(-6) \pm 5(-7)	1.1(-5) \pm 9(-7)	1.5(-5) \pm 1(-6)
L	N	2.9(-5) \pm 2(-6)	1.6(-4) \pm 3(-6)	5.1(-4) \pm 6(-6)	7.7(-4) \pm 8(-6)
R CrB	N	3.4(-5) \pm 2(-6)	2.5(-4) \pm 3(-6)	4.5(-4) \pm 6(-6)	5.2(-4) \pm 7(-6)
SN Ia		9(-7) \pm 3(-7)	1.7(-5) \pm 1(-6)	5.1(-5) \pm 2(-6)	1.4(-4) \pm 4(-6)
WD2 Merger		6.6(-5) \pm 2(-6)	4.3(-4) \pm 4(-6)	1.1(-3) \pm 9(-6)	1.5(-3) \pm 1(-5)

Table 4. The rate of mergers of binary WD formed via different evolutionary scenarii at 10 Gyr after an instantaneous star-formation burst as a function of $\alpha_{ce}\lambda$ (per $10^{10} M_{\odot} \text{yr}^{-1}$).

Scen.	$\alpha_{ce}\lambda$			
	0.25	0.5	1.0	2.0
1	-	-	-	9.8(-6) \pm 2(-6)
2	-	3.9(-6) \pm 7(-7)	1.3(-5) \pm 2(-6)	3.6(-5) \pm 4(-6)
3	9(-7) \pm 4(-7)	1.3(-5) \pm 1(-6)	2.5(-5) \pm 3(-6)	4.3(-5) \pm 5(-6)
4	-	-	1.1(-5) \pm 2(-6)	1.6(-5) \pm 3(-6)
5	-	1.1(-7) \pm 5(-8)	1.4(-6) \pm 7(-7)	7.2(-6) \pm 2(-6)
6	-	-	4.7(-7) \pm 4(-7)	2.1(-6) \pm 1(-6)
7	-	-	-	-
8	-	-	-	3.1(-5) \pm 4(-6)
SN Ia	9(-7) \pm 4(-7)	1.7(-5) \pm 1(-6)	5.1(-5) \pm 4(-6)	1.4(-4) \pm 9(-6)

Figure 2 shows the model DTD for the mergers of WDs potentially leading to SNe Ia and empirical data for elliptical galaxies from Subaru/XMM-Newton Deep Survey (Totani et al. 2008), galaxy clusters (Maoz et al. 2010), and a sample of galaxies from SLOAN II Survey (Maoz et al. 2012). Clearly, none of the models fit observations at very early epochs ($\lesssim 500$ Myr). Only models for $\alpha_{ce}\lambda=2$ fit points at ≈ 1 and 8 Gyr of DTD derived for SLOAN II Survey which has very large time-bins and error bars. If we consider the DTD for galaxy clusters, at $\approx (7 - 10)$ Gyr, the difference approaches a factor close to 3-4. The main fraction of mergers occurs in the zones **A** and **E** of the $M_{\text{acc}} - M_{\text{don}}$ diagram. For illustration, at the request of the referee, in Fig. 3 we replot DTD for the $\alpha_{ce}\lambda=2$ case, showing data for the first (0.05–2) Gyr on a log-scale. Note that, while the lines for particular scenarios are quite irregular, the summary line shows a gradual growth of the rate of SNe Ia, mainly as a result of the smooth increase of mergers occurring in zone **E** (merger of CO WDs). Recall also, that at $t \lesssim 2$ Gyr a significant contribution to SNe Ia rate may provide a SD-channel, associated either with hydrogen or helium transfer (see e. g. Bours et al. 2013; Wang et al. 2009).

Figure 4 shows DTD for eight scenarios listed in Table 1 for the most prolific combination $\alpha_{ce}\lambda=2$. While at very early times, $t \lesssim 1$ Gyr, scenarios 2, 4 and 7 dominate, later, at $t \approx (3 - 10)$ Gyr, comparable contribution is, crudely, provided by scenarii 2, 3 and 8 (see also Table 3). Scenario 7 is associated with massive WDs, and there is only a very narrow ‘gap’ of initial separations for binaries with $M_1 \lesssim 4.5 M_{\odot}$ which just enables mergers in less than about 4 Gyr. It is important that in all scenarios one of the merging components is either a He WD or a CO WD which descended from a He star. Thus, the envelopes of WD always have certain amount of He, which *may* experience detonation and, under favourable conditions, trigger a detonation in an accreting WD.

As a complement to Fig. 2, in Table 3 we present the rate of WD mergers occurring at 10 Gyr after star formation burst in different regions of the $M_{\text{acc}} - M_{\text{don}}$ diagram, while the rates of WD mergers at 10 Gyr after the burst as a function of $\alpha_{ce}\lambda$ are presented in Table 4.

Figures 1 – 4 and Tables 3 and 4 suggest that a satisfactory reproduction of the extant data on the DTD at $t \gtrsim$ several 100 Myr requires comparable contributions of

mergers of pairs of CO+CO WDs with $M_1 + M_2 \gtrsim M_{Ch}$ and mergers of $M_1 + M_2 \lesssim M_{Ch}$ pairs with CO WD accretors and very massive He or hybrid WD donors. Basically, this agrees with the proportions of $\sim M_{Ch}$ and sub- M_{Ch} SNe Ia inferred from consideration of the solar abundance of manganese (Seitenzahl et al. 2013) and from the analysis of the mass of SNe Ia ejecta (Scalzo et al. 2014a,b; Childress et al. 2015), see Discussion section. Note also that in the lower right panel of Fig.2 the model results for zone **E**, namely mergers of CO+CO WD pairs with $M_1 \geq 0.8 M_\odot$ and $M_2 \geq 0.6 M_\odot$ taken alone, also fit, within errors, observational data of (Maoz et al. 2012) for the 500 Myr–2.5 Gyr and 2.5 Gyr–12 Gyr time bins.

However, mergers of sub- M_{Ch} pairs occur predominantly in zone **A** of the $M_{acc} - M_{don}$ diagram. Surface detonations are likely to occur only if $M_1 \gtrsim 0.8 M_\odot$ (Guillochon et al. 2010; Dan et al. 2012).

If the first detonation occurs in the post-merger phase, further evolution resembles that of double-detonation systems, where detonation in the envelope plays the role of the trigger, as also noted by Dan et al. (2015). For the latter scenario, it was found that, for explosion to resemble a SN Ia, M_1 should be $\gtrsim 0.9 M_\odot$ (Sim et al. 2010). In our simulations for $\alpha_{ce}\lambda=2$, in the case of an instantaneous star formation burst, the fraction of accretors with $M_1 \gtrsim 0.8 M_\odot$ in the systems merging in zone **A** is, at $t \approx 10$ Gyr, close to 20 per cent. It is close to 40 per cent at $t \approx 8$ Gyr and much lower at other epochs. In the case of SFR described by Eq. (4) it is permanently close to 15 per cent, see below. If the stars that do not explode in the merger process also do not explode later, above-mentioned M_1 limits, if confirmed in future, may strongly reduce possible contribution of zone **A** to the rate of SN Ia.

Figures 5 and 6 illustrate evolution with time of the distribution of masses of accretors, donors and of total mass of the systems at merger for the case of instantaneous star-formation burst. Figure 6 shows these parameters for three time-bins. The average mass of accretors slightly increases with time: $M_1 \gtrsim 0.8 M_\odot$ have 40 per cent of them at (0–1) Gyr, 50 per cent at (5–6) Gyr, and 70 per cent at (10–11) Gyr. About 50 per cent of the donors have mass $\lesssim 0.6 M_\odot$ at any epoch; the other 50 per cent are more massive. Recall that WD with mass $\gtrsim 0.6 M_\odot$ have only traces of He at the surface. Sub- M_{Ch} total mass have 60 per cent of pairs at $t \lesssim 6$ Gyr and 40 per cent at later time. On the other hand, because the maximum mass of He WD is close to $0.47 M_\odot$, Fig. 5 strongly indicates that the majority of donors in merging systems are hybrid WD.

In Fig. 7 we show the evolution of the rate of WD mergers potentially leading to SNe Ia for a galaxy mimicking the Milky Way, with SFR given by Eq. (4). Dependence of the rate of SNe Ia on $\alpha_{ce}\lambda$ for different scenarios and zones of Fig. 1 is presented in tables 5 and 6, respectively. It is clear that, as in the case of star-formation burst, the rate of mergers increases with $\alpha_{ce}\lambda$, because less systems merge in CEs. The rate of putative SNe Ia slightly declines with time. This reflects declining SFR and the fact that, in all most prolific scenarios, mergers of DD peak at $\lesssim 1$ Gyr and then decline rather fast. Our estimate of the possible Galactic SNe Ia rate owing to DD mechanism, namely $6.5 \times 10^{-3} \text{ yr}^{-1}$ (for the mass of the bulge and thin disk equal to $7.2 \times 10^{10} M_\odot$) is close to the latest estimate presented in the literature,

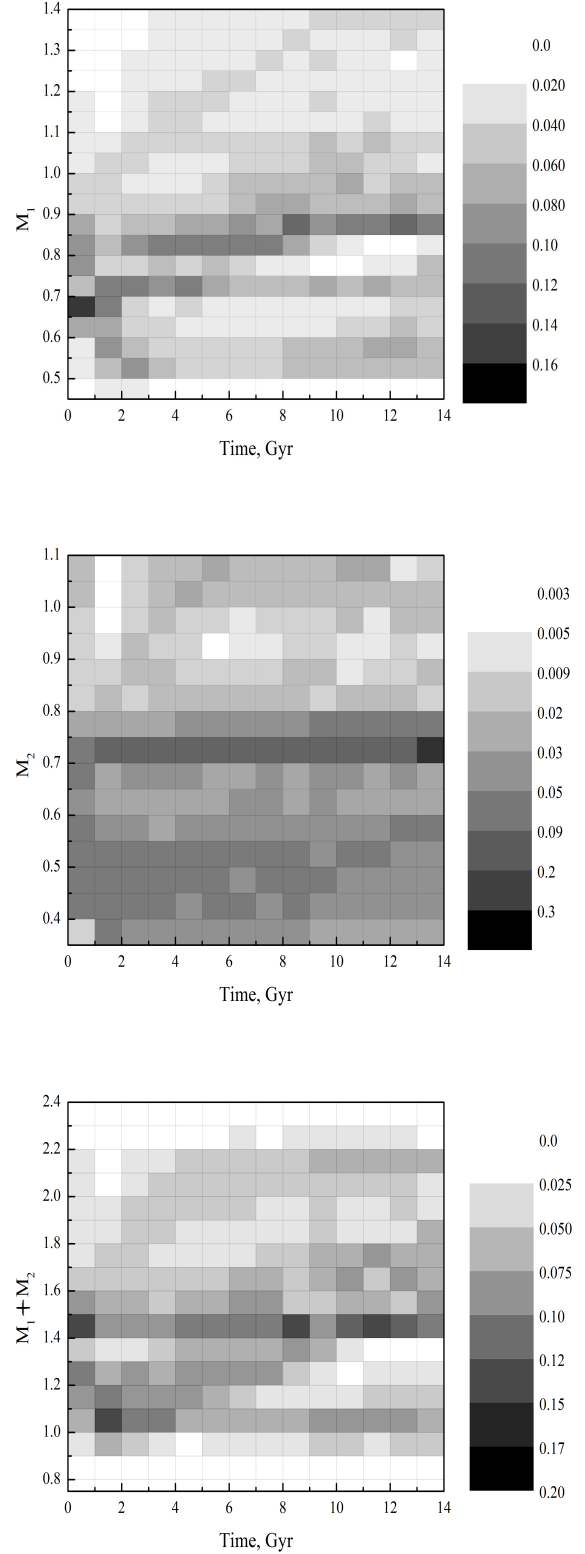


Figure 5. Distribution of masses of accretors (upper panel), donors (middle panel) and total mass (lower panel) of merging WD versus time after an instantaneous burst of star formation. Every time-bin is normalized to 1.

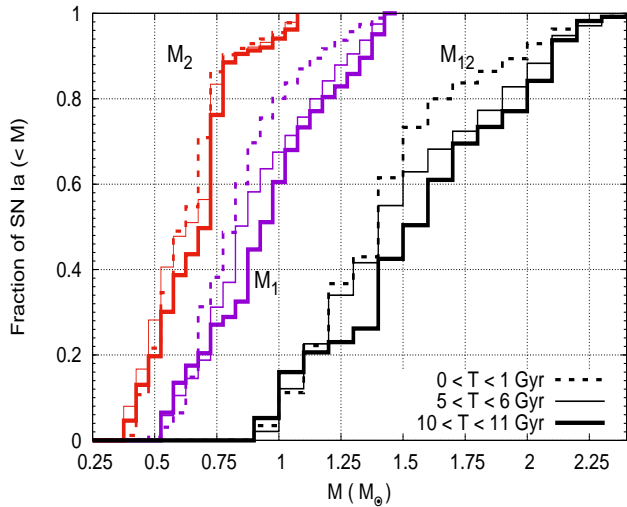


Figure 6. Distribution of M_1 , M_2 , and $M_1 + M_2$ (annotated as M_{12}) at three different epochs of the evolution of the ‘star-burst’ galaxy, shown in Fig. 5. Dotted lines: $0 \leq t \leq 1$ Gyr, thin solid lines: $5 \leq t \leq 6$ Gyr, thick solid lines: $10 \leq t \leq 11$ Gyr.

Table 5. The rate of mergers of binary WDs resulting in SN Ia formed via different evolutionary channels at $t = 14$ Gyr as a function of $\alpha_{ce}\lambda$ (per $10^{10}M_{\odot}\text{yr}^{-1}$). The star formation rate follows Eq. (4). The errors are negligibly small compared with rates.

Scenario	$\alpha_{ce}\lambda$			
	0.25	0.5	1.0	2.0
1	-	5.3(-7)	9.0(-6)	2.8(-5)
2	2.9(-6)	2.1(-5)	7.2(-5)	2.1(-4)
3	4.3(-5)	9.9(-5)	9.2(-5)	5.5(-5)
4	2.4(-7)	1.8(-6)	5.5(-5)	2.6(-4)
5	4.7(-8)	1.3(-6)	1.2(-5)	6.3(-5)
6	-	3.1(-7)	9.1(-6)	3.5(-5)
7	-	-	-	8.5(-5)
8	-	-	9.7(-7)	1.1(-4)
SN Ia	4.7(-5)	1.2(-4)	2.5(-4)	9.0(-4)

namely, $(5.4 \pm 0.12) \times 10^{-3} \text{ yr}^{-1}$ (with systematic factor ~ 2 ; Li et al. (2011)). Recall, however, that we employ an extreme assumption that *all* the following contribute to SNe Ia: mergers of super-Chandrasekhar pairs of CO WDs, mergers of CO WDs more massive than $0.47 M_{\odot}$ with hybrid or helium WDs more massive than $0.37 M_{\odot}$ and mergers of ONe and massive ($\geq 0.9 M_{\odot}$) CO WDs (Fig. 1). An increase of these limits, will reduce obtained rate.

The masses of accretors have a peak close to $0.7 M_{\odot}$ at $t = (1 - 7)$ Gyr after beginning of star formation in the bulge and thin disk and range, predominantly between $0.45 M_{\odot}$ and $1 M_{\odot}$ (Fig. 8). Later, average M_1 values very smoothly become lower and at the current assumed age of the Galaxy (14 Gyr) most of the accretor masses are between 0.6 and $1.0 M_{\odot}$. Donor masses have two peaks – close to $0.7 M_{\odot}$ (CO WD) and at $0.4 M_{\odot}$ to $0.6 M_{\odot}$ (most massive He WD and hybrid WD). The existence of two peaks in donor masses results in a double-peaked distribution of

Table 6. The rate of mergers of binary WDs resulting in SNe Ia formed via different evolutionary channels and occurring in different regions of the $M_{acc} - M_{don}$ diagram at $t = 14$ Gyr as a function of $\alpha_{ce}\lambda$ (per $10^{10}M_{\odot}\text{yr}^{-1}$). Star formation rate follows Eq. (4). Row ‘SN Ia’ provides the rate of potential SN Ia, while row ‘WD2’ shows the total rate of WD mergers.

Zone	DD	$\alpha_{ce}\lambda$			
		$M_{accret} - M_{don}$	0.25	0.5	1.0
A	Y	1.5(-5)	5.7(-5)	1.0(-4)	4.5(-4)
B	Y	5.8(-6)	3.9(-6)	1.1(-5)	6.8(-5)
C	N	1.4(-6)	1.3(-5)	3.2(-5)	8.4(-5)
D	Y	6.4(-7)	5.2(-6)	2.0(-5)	8.4(-5)
E	Y	1.8(-5)	3.1(-5)	9.1(-5)	2.4(-4)
F	Y	5.6(-7)	1.2(-6)	3.0(-6)	1.9(-5)
G	N	8.2(-9)	5.9(-6)	5.5(-5)	5.7(-5)
H	N	1.2(-7)	1.3(-7)	7.7(-7)	3.9(-5)
I	N	1.1(-5)	3.3(-5)	6.4(-5)	1.3(-4)
J	Y	5.2(-6)	9.1(-6)	2.2(-5)	4.6(-5)
K	N	4.8(-6)	2.6(-5)	4.4(-5)	4.4(-5)
L	N	9.7(-5)	2.2(-4)	6.4(-4)	1.0(-3)
R CrB	N	4.7(-5)	4.6(-4)	1.4(-3)	1.7(-3)
SN Ia		4.7(-5)	1.2(-4)	2.5(-4)	9.0(-4)
WD2		2.1(-4)	8.6(-4)	2.4(-3)	4.0(-3)

total mass of merging WDs, with peaks close to $1.0 M_{\odot}$ and $1.4 M_{\odot}$.

5 DISCUSSION

5.1 Tidal effects

A substantial uncertainty in the results of BPS for putative precursors of SNe Ia is caused by the treatment of tidal effects. As noted in § 3.1, they are not always taken into account, in contrast to our study. In order to illustrate the effect of tides, we present in Fig. 9 a model DTD obtained using the same BPS code, but excluding tidal effects and compare it with the model DTD obtained ‘with tides’ and with observations, as in Fig. 2. We present only summary curves. It is immediately clear that in the extreme case of absence of tides, the DTD becomes more compatible with observations, at least for the DTD derived from SNe Ia in the Subaru/XMM Survey by Totani et al. (2008) (diamonds) and in galaxy clusters by Maoz et al. (2010) (triangles). For comparison, we also show that, if as an extreme assumption we suppose that *all* merging WD produce SNe Ia, the rate of the latter due to DD-scenario becomes even higher than observed. The reason for better agreement with observations may be understood as the effect of typically later RLOF in the same systems and production of more massive WD. Some systems experience case C of mass exchange instead of case B.

5.2 Metallicity

Another source of uncertainty is stars with sub-solar metallicity: $Z \sim 0.0001$ may be typical for the first generation of stars enriched by heavy elements produced in explosions of Pop. III stars (Smith et al. 2015). Even in the Galaxy about 10 ultra-low-metallicity ($[\text{Fe}/\text{H}] < -7$) stars are known

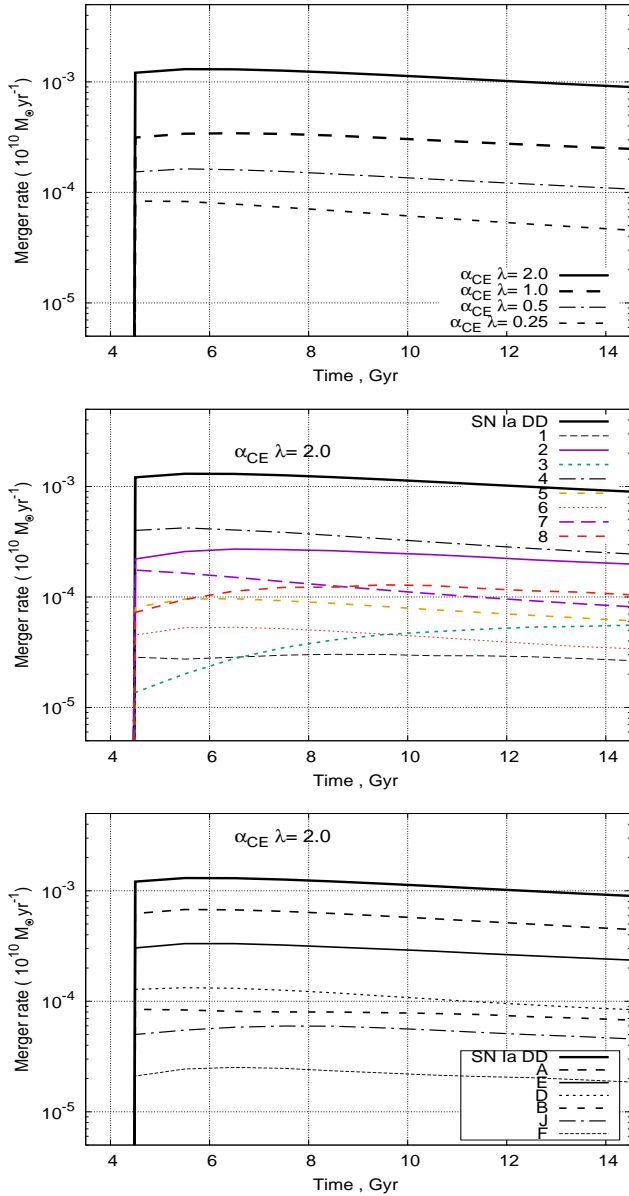


Figure 7. Evolution of the rate of WD mergers potentially leading to SNe Ia in the Galaxy, if star formation rate is set by Eq. (4). Upper panel: all potential SNe Ia as a function of $\alpha_{ce}\lambda$. Middle panel: systems produced by particular scenarios (Table 1). Lower panel: systems feeding different regions of the $M_{acc} - M_{don}$ diagram (Fig. 1).

(Keller et al. 2014). Reduction of Z to an extreme value of 0.0001 results in improvement of agreement with observational DTD (Fig. 2). The reason is a general increase of pre-contact masses of stars with decreasing Z , owing to strongly reduced stellar winds. However, this result should be taken with a pinch of salt: evolution of close binaries with non-solar Z in all BPS codes is an extrapolation of computations for $Z=0.02$. Because of different masses of stellar remnants at the end of similar evolutionary stages, the time-scales of evolution, further evolutionary scenarios and/or their relative significance may be different. In addition, the chemical

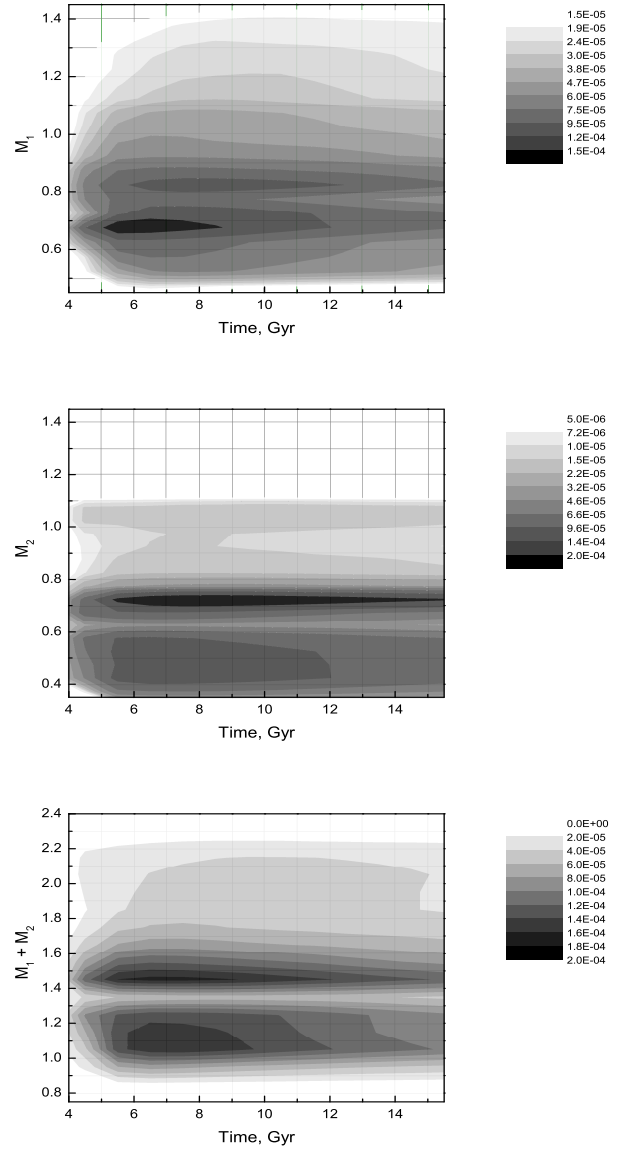


Figure 8. Distribution of masses of accretors (upper panel), donors (middle panel) and total mass (lower panel) of merging pairs of WDs potentially leading to SNe Ia versus time for a $10^{10} M_{\odot}$ galaxy with the star formation rate set by Eq. (4).

composition of WDs depends on their initial metallicity and may influence the development of explosions involving them.

5.3 Stability of mass-loss by the donors.

A long-standing problem is stability of mass-loss by donors with deep convective envelopes and in systems with high mass-ratio. In simulations, we used critical values of the mass-ratios of components for low-mass stars and giants implemented in BSE (Hurley et al. 2002, Eqs. (56), (57)), which allow stable mass loss by stars with deep convective envelopes only for $q_{cr} = M_{don}/M_{acc} \lesssim 1$, even if the donor has a condensed core. However, recent studies (Woods & Ivanova 2011; Passy et al. 2012) have shown that

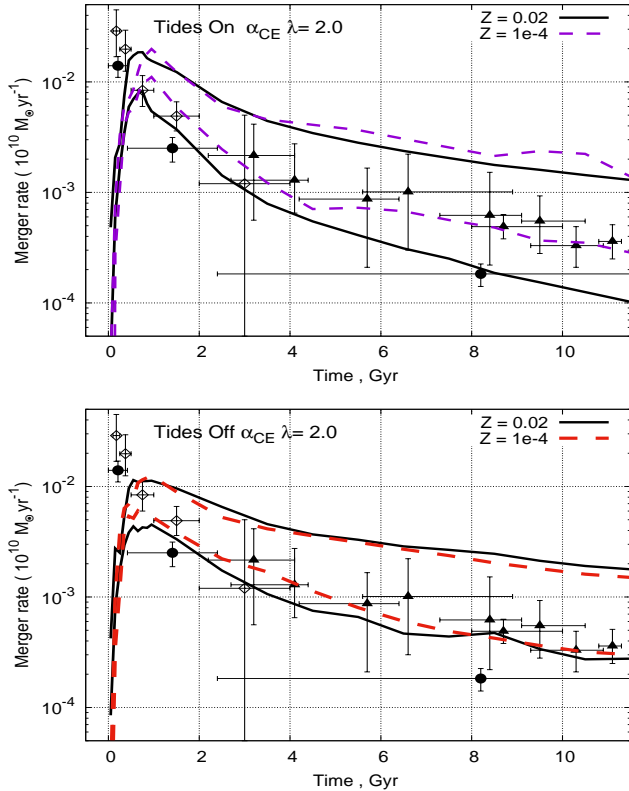


Figure 9. The effect of tides and abundance of metals on the DTD. Upper panel: lower solid line, DTD in the ‘standard’ model for $\alpha_{CE}\lambda=2$, $Z=0.02$ with tides taken into account; lower dashed line, DTD computed for the same model for $Z=0.0001$. The upper pair of lines shows the DTD for merger of *all* WD for two values of Z . Lower panel: the same distributions for the case when tidal effects are not taken into account. Observational data points are the same as in Fig. 2.

dynamical mass loss by red giants may be avoided owing to existence of a super-adiabatic outer layer of the giant’s envelope which has a local thermal time-scale comparable to the dynamical time-scale and has enough time to readjust thermally. Pavlovskii & Ivanova (2015) found that q_{cr} varies from 1.5 to 2.2 for conservative mass transfer⁵.

In scenarios 1 – 4 (Table 1), the first CO WD in the system forms via stable RLOF. For revised upward q_{cr} , more systems would avoid the first CE and, possibly, evolve to form a pair of WDs. Because typical separations of components after the second CE will be larger, a lower efficiency of matter ejection in CEs will be required for retaining or increase the rate of WD mergers.

5.4 Pre-CE core radii of the donors

Hall & Tout (2014) called attention to an uncertainty inherent to *all* BPS codes: it is unclear what values of radii is necessary to compare in order to find whether stars merged in CEs, namely, pre-CE core radii of the donors or the radii

⁵ Earlier, the possibility of $q_{cr} \simeq 2$ was found by Chen & Han (2008) in evolutionary computations, but no physical justification was provided.

of post-CE stripped remnants. Currently, in BSE the first option is implemented. As well, the radii of stellar cores themselves are poorly approximated. This uncertainty may influence, mostly, the outcome of CE produced by RLOF in the pairs of (i) HG and RGB, (ii) RGB and RGB stars, and (iii) in binaries harbouring HG or RGB stars with He WD companions. To test suggestion of Hall & Tout (2014), we implemented in the code suggested by them corrections for RGB and TPAGB stars. However, in our simulations we did not encounter events of the kinds (i) and (ii), while CEs with He WD are rather rare. Thus, our results remained virtually unaffected. The above-mentioned imperfections are partially outset by uncertainties in the core-envelope definition (i. e., envelope binding energy) and CE ejection efficiency. Hall & Tout noted that it is difficult to constrain the parameters found by them to be uncertain, by observations, since spatial densities of the concerned binaries are poorly known. All the above-mentioned problems in the treatment of binary star evolution still require a more systematic investigation before it will be possible to quantify the respective effects to the degree which will allow to make the necessary corrections in BPS codes. It is impossible to evaluate the influence of all of them on the rate of formation of putative progenitors of SNe Ia, but it may be easily suspected that, for example, the rates of merger of WDs will change within a factor of 2 – 3.

5.5 The slope of the DTD curve

The slope of DTD curve vs. the time close to t^{-1} is often considered as evidence in favour of DD- scenario being the main mechanism producing SNe Ia. If the distance between the components a after the last CE episode obeys the power-law $dN/da \propto a^\epsilon$, while the merger time depends on a as $t \propto a^\gamma$, the dependence of the DTD on time should be a power law with index $\phi = -1 + (\epsilon + 1)/\gamma$. It is usually assumed that merging pairs of WD are distributed over a like main sequence stars. Then $\phi = -1$, by virtue of almost ‘standard’ assumption $\epsilon = -1$ (Popova et al. 1982). In Fig. 10, we show distribution of progenitors of merging WD+WD binaries on the main sequence and before and after the last CE episode. It is clear that in the course of evolution distribution over a experiences complicated non-linear transformation and, separately, neither sub- M_{Ch} nor (super)- M_{Ch} mergers obey a a^{-1} law, but the latter is, crudely, followed by their combination. If other mechanisms also contribute to SNe Ia, they may also influence the slope of the DTD curve. The disagreement of the shape of model time-dependence of merging double-degenerates and a simple power-law was also noted by Ablimit et al. (2016).

5.6 The rate of SNe Ia.

The aim of our study was to estimate the upper bound to the input of mergers of WDs into the rate of SNe Ia. For a satisfactory agreement with observations, at least some of the included model events should be sub- M_{Ch} mergers, involving CO accretors and massive He WD or hybrid WD as donors. Observations provide some evidence in favour of existence of sub- M_{Ch} SNe Ia, through a significant scatter in the estimated masses of produced ⁵⁶Ni and ejected mass, which for

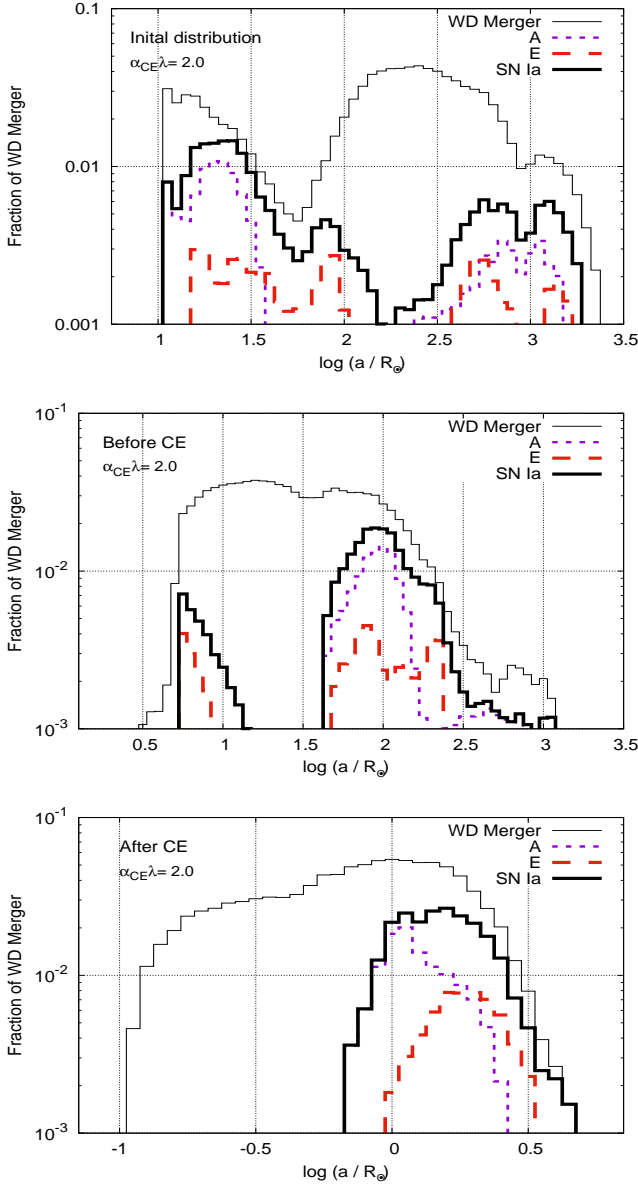


Figure 10. Distribution of separations of components of precursors of merging WD pairs $dN/d\log(a)$. The distribution is normalized to the total number of WD that merged over 10 Gyr (WD Merger in the legend). Upper panel, initial distribution. Middle panel, distribution before the last common envelope (CE) stage. Lower panel, distribution after the last CE.

some samples cluster around certain values, substantially below M_{Ch} (e. g., Stritzinger et al. 2006; Mazzali et al. 2007; Scalzo et al. 2014a,b; Childress et al. 2015). In particular, Scalzo et al. (2014a,b) claim that the fraction of sub- M_{Ch} SNe Ia may be up to 50 per cent. However, as yet, no conclusions are drawn, whether these features of SNe Ia are related to their mass or to variations in the explosion conditions of M_{Ch} WDs. On the other hand, our model sample of merging pairs of WDs contains a substantial fraction of strongly super- M_{Ch} pairs. As shown by Moll et al. (2014), however, the spectra of SNe Ia produced in these events resemble the spectra of ‘normal’ SNe Ia.

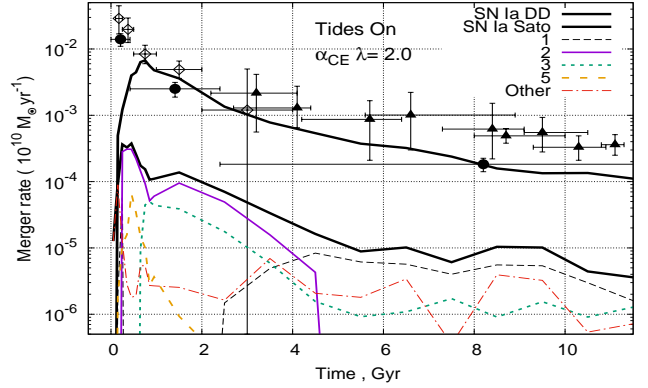


Figure 11. Upper solid line, DTD in the ‘standard’ model. Lower solid line, DTD for mergers of WD satisfying Eq. (1). The rest of the lines shows the contributions of particular scenarios, as in Fig. 4.

We have mentioned in comments to Figs. 2 and 4 that, within observational errors we get satisfactory agreement with observations even if we assume that only CO+CO WD pairs with $M_1 \geq 0.8 M_{\odot}$ and $M_2 \geq 0.6 M_{\odot}$ can produce SNe Ia. Here, we implicitly assumed that SNe Ia may explode either in the merger stage or in the merger product evolution stage. This issue is, however, still open. If we assume that explode pairs in which explosion conditions are met in the merger stage only and Eq. (1) should be satisfied, the expected rate of SNe Ia sharply drops. In Fig. 11 we compare observational DTD with model distribution for systems obeying Eq. (1). A reduction of the rate by a factor ~ 20 at $t = 10$ Gyr is immediately seen. This may signify serious problems either with observational estimates of DTD or in our understanding of processes that occur during and after mergers. It is interesting that scenario 3, which is one of the main contributors to the SNe Ia rate in the ‘standard’ model, in ‘Sato et al.’ case terminates production of massive mergers after ≈ 4 Gyr.

6 CONCLUSION

In the present study we have attempted to estimate the maximum possible contribution of merging binary WD to the total rate of SNe Ia. The main motivation of the study was the fact that, currently, merger of WDs is the only known (but still hypothetical) mechanism that has a natural time-scale overlapping with Hubble time. In our study we did not consider relations between different types of SNe Ia and possible combinations of components of the merging pairs, as we clearly recognize that there are ‘grey zones’ in which current simulations of mergers do not demonstrate events that are similar to SNe Ia of any known kind. This may be related to inaccessibility of the physical conditions necessary for SNe Ia explosions or be a result of an inadequate understanding of the physics, or of numerical problems. The only limits imposed on the components of merging pairs arise from the knowledge that merger results at least in a single detonation which may be treated as a transient event.

We found the most common scenarios of close binary

star evolution that result in formation of merging pairs of WDs and studied dependence of their relative role on the still cryptic parameters of binding energy of the stellar envelopes (λ) and efficiency of expulsion of matter in the CE stages (α_{ce}). We parametrized scenarios by the product $\alpha_{ce}\lambda$, which we varied from 0.25 to 2.0. We found, in agreement with some earlier studies (e. g., [Mennekens et al. 2010](#); [Toonen et al. 2012](#); [Ruiter et al. 2013](#); [Claeys et al. 2014](#)), that most merging pairs have stable RLOF as the first stage of mass transfer. At low $\alpha_{ce}\lambda$ the dominant scenarios are those in which the first RLOF occurs when the primary star overflows Roche lobe in the Hertzsprung gap or in the red giant stage. For larger $\alpha_{ce}\lambda$, scenarios in which the first RLOF happens in EAGB or TPAGB stages start to play role. It is important, that in about 50 per cent of merging pairs of WDs at least one of components is a He or a hybrid CO WD. The latter, in fact, dominate. The presence of at least traces of He at the surface of WDs may facilitate explosion at merger. With increase of $\alpha_{ce}\lambda$, the role of different scenarios becomes more even.

With an increase of $\alpha_{ce}\lambda$ from 0.25 to 2, the total rate of mergers increases. If $\alpha_{ce}\lambda$ is low, a large fraction of systems merges in CE. If this product of model parameters is high, a significant fraction of WD+WD pairs is too wide to merge in Hubble time.

We compared the model DTD with results derived from observations of several samples of SNe Ia. In the model, we consider the mergers singled out in $M_{acc} - M_{don}$ diagram as precursors of SNe Ia. The best agreement with observations was obtained for high $\alpha_{ce}\lambda=2$. Within observational errors, at $1 \lesssim t \lesssim 8$ Gyr, the model DTD for all mergers agrees with DTD derived by [Totani et al. \(2008\)](#); [Maoz et al. \(2010, 2012\)](#). For earlier epochs, model DTD has about 3 times less events than observed DTD. For $t \approx 10$ Gyr, the discrepancy with the data of [Maoz et al. \(2012\) is \$\simeq 4\$. If we take into account only ‘canonical’ mergers of CO+CO WDs with \$M_1 + M_2 \geq 1.4\$, the model DTD is still roughly comparable with the lowest observational DTD estimates for field galaxies \(\[Maoz et al. 2012\]\(#\)\), as in the studies of \[Ruiter et al. \\(2013\\)\]\(#\); \[Claeys et al. \\(2014\\)\]\(#\)⁶, but SNe Ia rates are higher than in the models of \[Ablimit et al. \\(2016\\) in which a more stringent requirement, \\$M_1 + M_2 \geq 1.6 M_{\odot}\\$, \\$q > 0.8\\$, is applied. The current rate of SNe Ia in the Milky Way, if all mergers expected by us to result in SNe Ia of some kind really produce them, is \\$6.5 \times 10^{-3} \text{yr}^{-1}\\$, remarkably close to the observationally inferred estimate \\$\\(5.4 \pm 0.12\\) \times 10^{-3} \text{yr}^{-1}\\$. The model estimate may be lower if our Eq. \\(4\\) overestimates the actual Galactic *SFR* \\(see e. g. \\[Chomiuk & Povich 2011\\]\\(#\\)\\).\]\(#\)](#)

The transformations of the separation of components during evolution with RLOF and CEs are strongly non-linear. Different scenarios produce non-flat distributions over $\log(a)$ and their sum is also not flat. As a result, we find that the model DTD does not depend on time like power law with an exponent close to -1, as expected from simplified es-

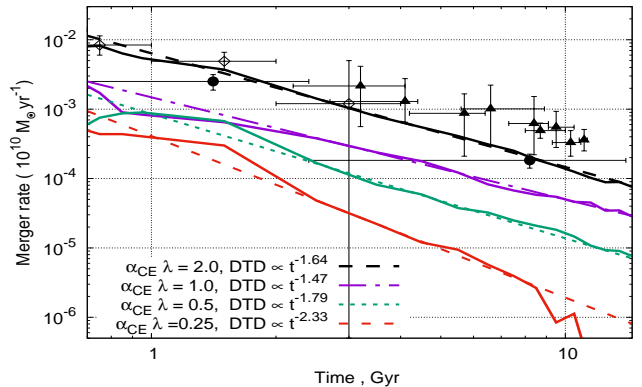


Figure 12. The slope of DTD for $t \geq 1$ Gyr, as in Fig. 2. Tides are accounted in the model, $Z=0.02$. Broken lines represent power-law approximations to DTD for different values of $\alpha_{ce}\lambda$.

timates, assuming that after the last CE episode distribution of separations of WD is flat in $\log(a)$. The slope of DTD in our models is a power law, depending on the assumed $\alpha_{ce}\lambda$ (Fig. 12). The exponents of power law range from -2.33 to -1.64 for $\alpha_{ce}\lambda$ from 0.25 to 2, respectively. The curve with the smallest absolute value of the exponent fits observations for $t \lesssim 8$ Gyr.

Our model does not fit [Maoz et al. \(2012\) bin of DTD at the shortest delay time, namely, \$t \lesssim 420\$ Myr. However, most SNe Ia in this time-bin may actually be produced by double-detonations. It was shown by \[Ruiter et al. \\(2014\\) that the double-detonation scenario involving non-degenerate donors and massive CO WD accretors reaches the peak at \\(200–300\\) Myr and extends to about 500 Myr. At the peak, the rate of SNe Ia is \\$\\(3 - 4\\) \times 10^{-3}\\$ per \\$10^{10} M_{\odot} \text{yr}^{-1}\\$. DTD of \\[Ruiter et al. \\\(2014\\\) has a second peak, comparable in maximum rate and extending to several Gyr. It is produced by the systems with long-living degenerate He-donors \\\(AM CVn stars\\\). However, it was shown by \\\[Piersanti et al. \\\\(2015\\\\) that in such systems outbursts of He burning never become dynamical and, respectively, AM CVn stars with He WD donors produce neither ‘regular’ SNe Ia nor lower scale SNe Ia. Thus, this scenario can not play any role in early-type galaxies with majority of stars formed in the initial spike of star formation. For the earliest epochs, inclusion of both SNe Ia of double-degenerate origin and double-detonation SNe Ia may reduce the discrepancy between observations and model.\\\]\\\(#\\\)\\]\\(#\\)\]\(#\)](#)

Some evidence in favour of the existence of sub- M_{Ch} SNe Ia is not related directly to interpretation of their observations. As noted above, [Seitenzahl et al. \(2013\)](#) noticed that manganese is produced efficiently in explosions only of WDs close to M_{Ch} . The observed $[\text{Mn}/\text{Fe}]$ ratio in solar neighbourhood may be reproduced, if about half of SNe Ia involve near- M_{Ch} WD, while the rest may be sub- M_{Ch} . However, this conclusion does not restrict the mechanism of sub- M_{Ch} SNe Ia. [Badenes & Maoz \(2012\)](#) estimated the merger rate of Galactic binary WD and found that it is rather similar to the inferred rate of SNe Ia in the Milky Way-like Sbc galaxies. They concluded that there are not nearly enough super- M_{Ch} pairs of WDs to reproduce this

⁶ Actually, this is not surprising, since the codes used by [Toonen et al. \(2012\)](#); [Ruiter et al. \(2013\)](#); [Claeys et al. \(2014\)](#) are based on the same system of evolutionary tracks as BSE code; the difference between codes is, as mentioned in the text, in the treatment of evolution of binaries ([Toonen et al. 2014](#)).

rate and, therefore, sub- M_{Ch} pairs may be partially responsible for the SNe Ia rate.

One prediction of single-degenerate models with non-degenerate donors is sweeping of H- or He-rich material from the envelope of the donor by the SN ejecta. Up to now, 17 ‘normal’ SNe Ia have been surveyed for swept-up matter. The upper limits on the amount of the latter are inconsistent with MS/RG donor (see Maguire et al. 2016, and references therein). On the other hand, as noted by Shen et al. (2013), nascent He WDs have thin H-envelopes which, in the case of merging WDs, will be transferred stably onto CO accretor prior to tidal disruption of the He-core of the donor. This hydrogen is likely to be ejected from the binary in Novae eruptions and sweep-up the surrounding ISM hundreds to thousands of years prior to a possible SN Ia. As found by Shen et al. (2013), it may create ISM profiles closely matching those, inferred from observations of some SNe Ia. As well, interaction of tidal tails with ISM may create NaI D-line profiles similar to those observed (Raskin & Kasen 2013). Thus, observations of narrow absorption lines from circumstellar medium do not necessarily manifest the presence of a non-degenerate component in a pre-SN Ia binary.

On the other hand, the existence of a single-degenerate channel to SN Ia may be signified by enhanced brightness and blue and ultraviolet emission arising when the ejected material interacts with companion star Kasen (2010). UV-emission bursts were recently observed in the early spectra of several SNe Ia (Cao et al. 2015; Im et al. 2015; Marion et al. 2016). However, interpretation of their observations as manifestation of SD-scenario is still a matter of debate (Liu & Stancliffe 2016; Kromer et al. 2016). For a variety of SD-scenario – SNe Ia in symbiotic systems – Chomiuk et al. (2016), based on radio-observations, limit the fraction of SNe Ia in systems with red giant components to $\lesssim 10$ per cent. Strong evidence for Chandrasekhar-mass explosions is provided by observations of SN remnant 3C 397 (Yamaguchi et al. 2015) for which Ni/Fe and Mn/Fe mass ratios derived from X-ray observations are consistent only with nucleosynthesis processes occurring in near- M_{Ch} SN.

It would be incorrect to blame population synthesis alone for the mismatch of models and observations. As we noted in § 2, SPH simulations of merger process suffer from insufficient resolution. Increase of the latter will allow us to resolve smaller hot regions, thus allowing better understanding of conditions for detonation at contact, especially in the systems with He-rich donors. DTD, in turn, are uncertain by almost an order of magnitude, as seen in the Figures above; almost certainly this is not an effect of different methods applied for their recovery, but also an effect of dependence of samples of SNe Ia under study on the environment.

We have shown that by accounting for all WD merger events that hypothetically *may* produce SNe Ia either during merger processes or in the course of further evolution, it is possible within reasonable limits to explain the DTD for SNe Ia and the rate of SN Ia in the Milky Way. However, the diversity of combinations of chemical composition of components of merging pairs and their masses leaves open the question, why majority of SNe Ia are so ‘standard’.

The authors acknowledge the referee for his/her valuable comments. We appreciate helpful discussions with M.

Dan, N. Chugai, G. Nelemans, K. Postnov, S. Toonen, H.-L. Chen. D. Kolesnikov is acknowledged for trial computations of evolutionary sequences for helium stars. We acknowledge J. Hurley and his co-authors for making the code BSE public. The study was partially supported by Basic Research Program P-7 of the Praesidium of the Russian Academy of Sciences and Russian Foundation for Basic Research (contracts No. 14-12-00146 and 14-02-00657). AGK acknowledges support from M.V. Lomonosov Moscow State University Program of Development. This research has made use of NASAs ADS Bibliographic Services.

REFERENCES

- Ablimit I., Maeda K., Li X.-D., 2016, *ApJ*, **826**, 53
 Badenes C., Maoz D., 2012, *ApJ*, **749**, L11
 Bours M. C. P., Toonen S., Nelemans G., 2013, *Astron.Astrophys.*, **552**, A24
 Brooks J., Bildsten L., Marchant P., Paxton B., 2015, *ApJ*, **807**, 74
 Bulla M., Sim S. A., Pakmor R., Kromer M., Taubenberger S., Röpke F. K., Hillebrandt W., Seitenzahl I. R., 2016, *MNRAS*, **455**, 1060
 Burkart J., Quataert E., Arras P., Weinberg N. N., 2013, *MNRAS*, **433**, 332
 Camacho J., Torres S., García-Berro E., Zorotovic M., Schreiber M. R., Rebassa-Mansergas A., Nebot Gómez-Morán A., Gänsicke B. T., 2014, *Astron.Astrophys.*, **566**, A86
 Cao Y., et al., 2015, *Nature*, **521**, 328
 Chen X., Han Z., 2002, *MNRAS*, **335**, 948
 Chen X., Han Z., 2008, *MNRAS*, **387**, 1416
 Childress M. J., et al., 2015, *MNRAS*, **454**, 3816
 Chomiuk L., Povich M. S., 2011, *AJ*, **142**, 197
 Chomiuk L., et al., 2016, *ApJ*, **821**, 119
 Claeys J. S. W., Pols O. R., Izzard R. G., Vink J., Verbunt F. W. M., 2014, *Astron.Astrophys.*, **563**, A83
 D’Souza M., Motl P., Tohline J., J. F., 2006, *ApJ*, **643**, 381
 Dan M., Rosswog S., Brügggen M., 2009, *Journal of Physics Conference Series*, **172**, 012034
 Dan M., Rosswog S., Guillochon J., Ramirez-Ruiz E., 2011, *ApJ*, **737**, 89
 Dan M., Rosswog S., Guillochon J., Ramirez-Ruiz E., 2012, *MNRAS*, **422**, 2417
 Dan M., Rosswog S., Brügggen M., Podsiadlowski P., 2014, *MNRAS*, **438**, 14
 Dan M., Guillochon J., Brügggen M., Ramirez-Ruiz E., Rosswog S., 2015, *MNRAS*, **454**, 4411
 Dubey A., Reid L. B., Weide K., Antypas K., Ganapathy M. K., Riley K., Sheeler D., Siegal A., 2009, preprint, ([arXiv:0903.4875](https://arxiv.org/abs/0903.4875))
 Fryxell B., et al., 2000, *ApJS*, **131**, 273
 Fuller J., Lai D., 2012, *MNRAS*, **421**, 426
 Gilmore G., 2001, in J. G. Funes & E. M. Corsini ed., *Astronomical Society of the Pacific Conference Series Vol. 230, Galaxy Disks and Disk Galaxies*. pp 3–12
 Guerrero J., García-Berro E., Isern J., 2004, *Astron.Astrophys.*, **413**, 257
 Guillochon J., Dan M., Ramirez-Ruiz E., Rosswog S., 2010, *ApJ*, **709**, L64
 Hall P. D., Tout C. A., 2014, *MNRAS*, **444**, 3209
 Hillebrandt W., Kromer M., Röpke F. K., Ruiter A. J., 2013, *Frontiers of Physics*, **8**, 116
 Holcomb C., Guillochon J., De Colle F., Ramirez-Ruiz E., 2013, *ApJ*, **771**, 14
 Hoyle F., Fowler W. A., 1960, *ApJ*, **132**, 565
 Hurley J. R., Pols O. R., Tout C. A., 2000, *MNRAS*, **315**, 543

- Hurley J. R., Tout C. A., Pols O. R., 2002, *MNRAS*, 329, 897
- Hut P., 1981, *Astron.Astrophys.*, 99, 126
- Iben I. J., 1986, *ApJ*, 304, 201
- Iben I., Tutukov A. V., 1984, *ApJS*, 54, 335
- Iben I., Tutukov A. V., 1985, *ApJS*, 58, 661
- Iben I. J., Tutukov A. V., 1991, *ApJ*, 370, 615
- Iben I. J., Tutukov A. V., Yungelson L. R., 1996, *ApJ*, 456, 750
- Ilkov M., Soker N., 2012, *MNRAS*, 419, 1695
- Im M., Choi C., Yoon S.-C., Kim J.-W., Ehgamberdiev S. A., Monard L. A. G., Sung H.-I., 2015, *ApJS*, 221, 22
- Ivanova N., et al., 2013, *A&ARv*, 21, 59
- Ji S., et al., 2013, *ApJ*, 773, 136
- Jorgensen H. E., Lipunov V. M., Panchenko I. E., Postnov K. A., Prokhorov M. E., 1997, *ApJ*, 486, 110
- Kasen D., 2010, *ApJ*, 708, 1025
- Kashi A., Soker N., 2011, *MNRAS*, 417, 1466
- Kashyap R., Fisher R., García-Berro E., Aznar-Siguán G., Ji S., Lorén-Aguilar P., 2015, *ApJ*, 800, L7
- Katz M. P., Zingale M., Calder A. C., Swesty F. D., Almgren A. S., Zhang W., 2016, *ApJ*, 819, 94
- Keller S. C., et al., 2014, *Nature*, 506, 463
- Kiel P. D., Hurley J. R., Bailes M., Murray J. R., 2008, *MNRAS*, 388, 393
- Kitaura F. S., Janka H.-T., Hillebrandt W., 2006, *Astron.Astrophys.*, 450, 345
- Klypin A., Zhao H., Somerville R. S., 2002, *ApJ*, 573, 597
- Kromer M., et al., 2016, *MNRAS*, 459, 4428
- Levanon N., Soker N., García-Berro E., 2015, *MNRAS*, 447, 2803
- Li W., Chornock R., Leaman J., Filippenko A. V., Poznanski D., Wang X., Ganeshalingam M., Mannucci F., 2011, *MNRAS*, 412, 1473
- Liu Z.-W., Stancliffe R. J., 2016, *MNRAS*, 459, 1781
- Livne E., Glasner A., 1991, *ApJ*, 370, 272
- Maguire K., Taubenberger S., Sullivan M., Mazzali P. A., 2016, *MNRAS*, 457, 3254
- Maoz D., Sharon K., Gal-Yam A., 2010, *ApJ*, 722, 1879
- Maoz D., Mannucci F., Brandt T. D., 2012, *MNRAS*, 426, 3282
- Maoz D., Mannucci F., Nelemans G., 2014, *ARA&A*, 52, 107
- Marion G. H., et al., 2016, *ApJ*, 820, 92
- Marquardt K. S., Sim S. A., Ruiter A. J., Seitzzahl I. R., Ohlmann S. T., Kromer M., Pakmor R., Röpke F. K., 2015, *Astron.Astrophys.*, 580, A118
- Marsh T. R., Nelemans G., Steeghs D., 2004, *MNRAS*, 350, 113
- Mazzali P. A., Röpke F. K., Benetti S., Hillebrandt W., 2007, *Science*, 315, 825
- McKernan B., Ford K. E. S., 2016, *MNRAS*,
- Mennekens N., Vanbeveren D., De Greve J. P., De Donder E., 2010, *Astron.Astrophys.*, 515, A89+
- Moll R., Raskin C., Kasen D., Woosley S., 2013, preprint, ([arXiv:1311.5008](https://arxiv.org/abs/1311.5008))
- Moll R., Raskin C., Kasen D., Woosley S. E., 2014, *ApJ*, 785, 105
- Nelemans G., Yungelson L. R., Portegies Zwart S. F., Verbunt F., 2001a, *Astron.Astrophys.*, 365, 491
- Nelemans G., Portegies Zwart S. F., Verbunt F., Yungelson L. R., 2001b, *Astron.Astrophys.*, 368, 939
- Nomoto K., 1982, *ApJ*, 257, 780
- Ohlmann S. T., Röpke F. K., Pakmor R., Springel V., 2016, *ApJ*, 816, L9
- Paczyński B., 1971, *Acta.Astron.*, 21, 1
- Pakmor R., Kromer M., Röpke F. K., Sim S. A., Ruiter A. J., Hillebrandt W., 2010, *Nature*, 463, 61
- Pakmor R., Kromer M., Taubenberger S., Sim S. A., Röpke F. K., Hillebrandt W., 2012, *ApJ*, 747, L10
- Pakmor R., Kromer M., Taubenberger S., Springel V., 2013a, *ApJ*, 770, L8
- Pakmor R., Kromer M., Taubenberger S., Springel V., 2013b, *ApJ*, 770, L8
- Passy J.-C., Herwig F., Paxton B., 2012, *ApJ*, 760, 90
- Pavlovskii K., Ivanova N., 2015, *MNRAS*, 449, 4415
- Piersanti L., Gagliardi S., Iben I. J., Tornambé A., 2003a, *ApJ*, 583, 885
- Piersanti L., Gagliardi S., Iben I. J., Tornambé A., 2003b, *ApJ*, 598, 1229
- Piersanti L., Tornambé A., Yungelson L. R., 2014, *MNRAS*, 445, 3239
- Piersanti L., Yungelson L. R., Tornambé A., 2015, *MNRAS*, 452, 2897
- Pols O. R., Schroder K., Hurley J. R., Tout C. A., Eggleton P. P., 1998, *MNRAS*, 298, 525
- Popova E. I., Tutukov A. V., Yungelson L. R., 1982, *Ap&SS*, 88, 55
- Postnov K. A., Yungelson L. R., 2014, *Living Reviews in Relativity*, 17, 3
- Raskin C., Kasen D., 2013, *ApJ*, 772, 1
- Raskin C., Timmes F. X., Scannapieco E., Diehl S., Fryer C., 2009, *MNRAS*, 399, L156
- Raskin C., Scannapieco E., Fryer C., Rockefeller G., Timmes F. X., 2012, *ApJ*, 746, 62
- Rosswog S., Ramirez-Ruiz E., Hix W. R., 2009a, *Journal of Physics Conference Series*, 172, 012036
- Rosswog S., Kasen D., Guillochon J., Ramirez-Ruiz E., 2009b, *ApJ*, 705, L128
- Ruiter A. J., Belczynski K., Fryer C., 2009, *ApJ*, 699, 2026
- Ruiter A. J., et al., 2013, *MNRAS*, 429, 1425
- Ruiter A. J., Belczynski K., Sim S. A., Seitzzahl I. R., Kwiatkowski D., 2014, *MNRAS*, 440, L101
- Ruiz-Lapuente P., 2014, *New Astron. Rev.*, 62, 15
- Ruiz-Lapuente P., Burkert A., Canal R., 1995, *ApJ*, 447, L69
- Sato Y., Nakasato N., Tanikawa A., Nomoto K., Maeda K., Hachisu I., 2015, *ApJ*, 807, 105
- Sato Y., Nakasato N., Tanikawa A., Nomoto K., Maeda K., Hachisu I., 2016, *The Astrophysical Journal*, 821, 67
- Savonije G. J., de Kool M., van den Heuvel E. P. J., 1986, *Astron.Astrophys.*, 155, 51
- Scalzo R., et al., 2014a, *MNRAS*, 440, 1498
- Scalzo R. A., Ruiter A. J., Sim S. A., 2014b, *MNRAS*, 445, 2535
- Schwab J., Shen K. J., Quataert E., Dan M., Rosswog S., 2012, *MNRAS*, 427, 190
- Schwab J., Quataert E., Kasen D., 2016, *MNRAS*, 463, 3461
- Seitzzahl I. R., Meakin C. A., Townsley D. M., Lamb D. Q., Truran J. W., 2009, *ApJ*, 696, 515
- Seitzzahl I. R., Cescutti G., Röpke F. K., Ruiter A. J., Pakmor R., 2013, *Astron.Astrophys.*, 559, L5
- Shara M. M., Hurley J. R., 2002, *ApJ*, 571, 830
- Shen K. J., Bildsten L., 2013, preprint, ([arXiv:1305.6925](https://arxiv.org/abs/1305.6925))
- Shen K. J., Bildsten L., 2014, *ApJ*, 785, 61
- Shen K. J., Moore K., 2014, *ApJ*, 797, 46
- Shen K. J., Kasen D., Weinberg N. N., Bildsten L., Scannapieco E., 2010, *ApJ*, 715, 767
- Shen K. J., Bildsten L., Kasen D., Quataert E., 2012, *ApJ*, 748, 35
- Shen K. J., Guillochon J., Foley R. J., 2013, *ApJ*, 770, L35
- Shigeyama T., Nomoto K., Yamaoka H., Thielemann F.-K., 1992, *ApJ*, 386, L13
- Sim S. A., Röpke F. K., Hillebrandt W., Kromer M., Pakmor R., Fink M., Ruiter A. J., Seitzzahl I. R., 2010, *ApJ*, 714, L52
- Smith B. D., Wise J. H., O'Shea B. W., Norman M. L., Khochfar S., 2015, *MNRAS*, 452, 2822
- Sparks W. M., Stecher T. P., 1974, *ApJ*, 188, 149
- Stritzinger M., Leibundgut B., Walch S., Contardo G., 2006, *Astron.Astrophys.*, 450, 241
- Sweigart A. V., Gross P. G., 1978, *ApJS*, 36, 405
- Taam R. E., 1980, *ApJ*, 242, 749
- Tanikawa A., Nakasato N., Sato Y., Nomoto K., Maeda K., Hachisu I., 2015, *ApJ*, 807, 40
- Tauris T., Dewi J. D. M., 2001, *â*, 369, 170

- Toonen S., Nelemans G., Portegies Zwart S., 2012, *Astron.Astrophys.*, **546**, A70
- Toonen S., Claeys J. S. W., Mennekens N., Ruiter A. J., 2014, *Astron.Astrophys.*, **562**, A14
- Totani T., Morokuma T., Oda T., Doi M., Yasuda N., 2008, *PASJ*, **60**, 1327
- Tout C. A., Aarseth S. J., Pols O. R., Eggleton P. P., 1997, *MNRAS*, **291**, 732
- Tutukov A. V., Yungelson L. R., 1979a, in de Loore C., Conti P. S., eds, *Mass loss and evolution of O-type stars*. Reidel, Dordrecht, p. 401
- Tutukov A. V., Yungelson L. R., 1979b, *Acta Astron.*, **29**, 665
- Tutukov A. V., Yungelson L. R., 1981, *Nauchnye Informatsii*, **49**, 3
- Tutukov A. V., Yungelson L. R., 1994, *MNRAS*, **268**, 871
- Waldman R., Sauer D., Livne E., Perets H., Glasner A., Mazzali P., Truran J. W., Gal-Yam A., 2011, *ApJ*, **738**, 21
- Wang B., Chen X., Meng X., Han Z., 2009, *ApJ*, **701**, 1540
- Webbink R. F., 1979, in *White Dwarfs and Variable Degenerate Stars*. pp 426–447
- Webbink R. F., 1984, *ApJ*, **277**, 355
- Woods T. E., Ivanova N., 2011, *ApJ*, **739**, L48
- Yamaguchi H., et al., 2015, *ApJ*, **801**, L31
- Yu S., Jeffery C. S., 2010, *Astron.Astrophys.*, **521**, A85+
- Yungelson L. R., 2008, *Astronomy Letters*, **34**, 620
- Yungelson L. R., Livio M., 2000, *ApJ*, **528**, 108
- Zahn J.-P., 1975, *Astron.Astrophys.*, **41**, 329
- Zhu C., Chang P., van Kerkwijk M. H., Wadsley J., 2013, *ApJ*, **767**, 164
- Zhu C., Pakmor R., van Kerkwijk M. H., Chang P., 2015, *ApJ*, **806**, L1
- Zorotovic M., Schreiber M. R., Gänsicke B. T., Nebot Gómez-Morán A., 2010, *Astron.Astrophys.*, **520**, A86
- de Kool M., 1990, *ApJ*, **358**, 189
- van Haaften L. M., Nelemans G., Voss R., Toonen S., Portegies Zwart S. F., Yungelson L. R., van der Sluys M. V., 2013, *Astron.Astrophys.*, **552**, A69
- van Kerkwijk M. H., Chang P., Justham S., 2010, *ApJ*, **722**, L157
- van Rossum D. R., Kashyap R., Fisher R., Wollaeger R. T., García-Berro E., Aznar-Siguán G., Ji S., Lorén-Aguilar P., 2016, *ApJ*, **827**, 128

APPENDIX A: SCENARI

Below, we show for scenarios 1 – 8 the initial distributions of the masses of components of the progenitor systems, the initial relations between masses of primaries and the separation of the components in these systems and the location of components of merging systems in the $M_{\text{acc}} - M_{\text{don}}$ diagram. Labels in the Figures correspond to Table 1.

In Tables A1-A8 we present for each scenario typical tracks leading to the merger, indicating evolutionary lifetime (T), evolutionary status of the components (Star1 and Star2), the filling factors of the respective Roche lobes (R1/RL1 and R2/RL2), the masses of the components (M1 and M2) and their separation A (in solar units). If filling factor is < 0.01 we assign to it, for brevity, the value of 0.0.

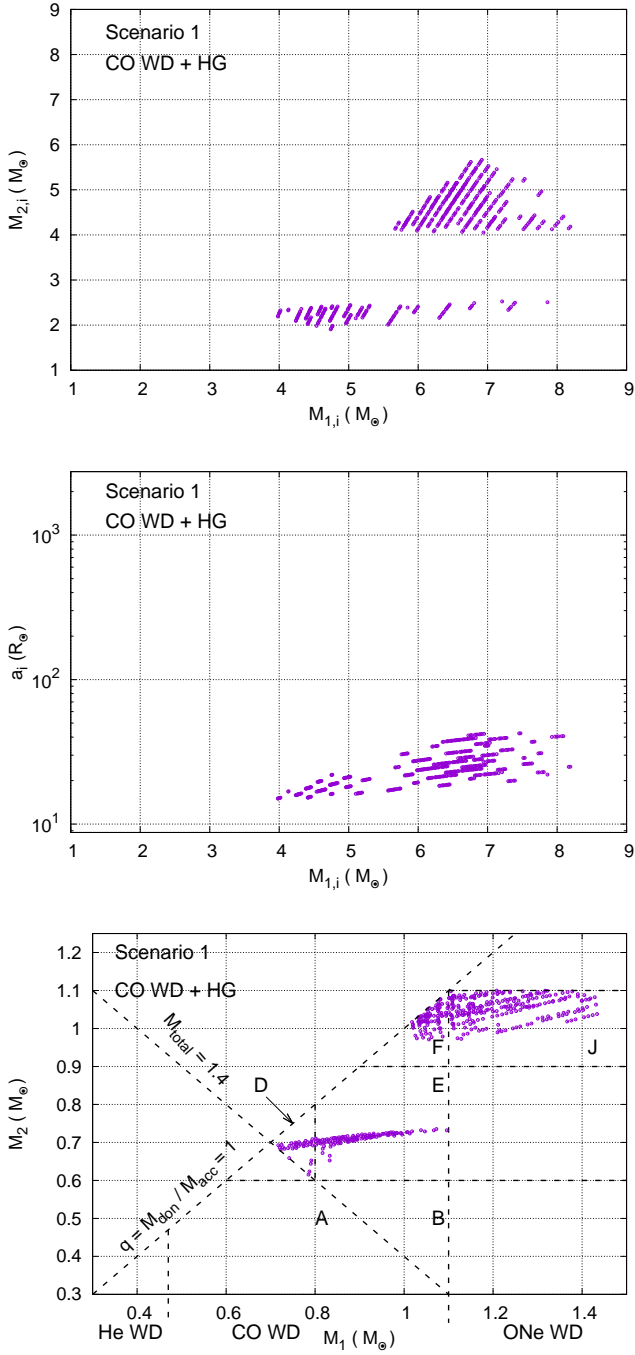


Figure A1. Close binaries evolving via scenario 1. Upper panel: initial distribution of the masses of the components. Middle panel: initial relationship between the masses of primaries and the separation of components. Lower panel: position of merging systems produced via scenario 1 in $M_{\text{acc}} - M_{\text{don}}$ diagram. The label in the Figure indicates evolutionary stage of the system prior to the first common envelope episode in the system as in Table 1.

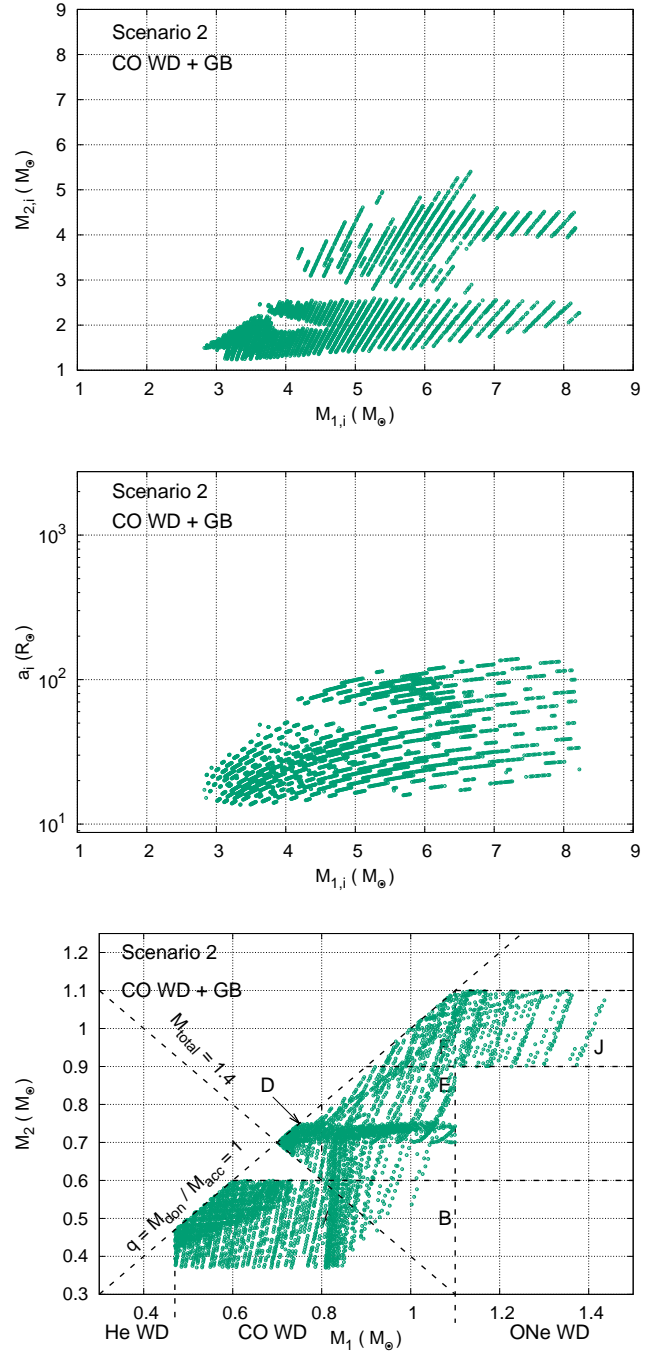


Figure A2. As Fig. A1, but for scenario 2.

This paper has been typeset from a $\text{\TeX}/\text{\LaTeX}$ file prepared by the author.

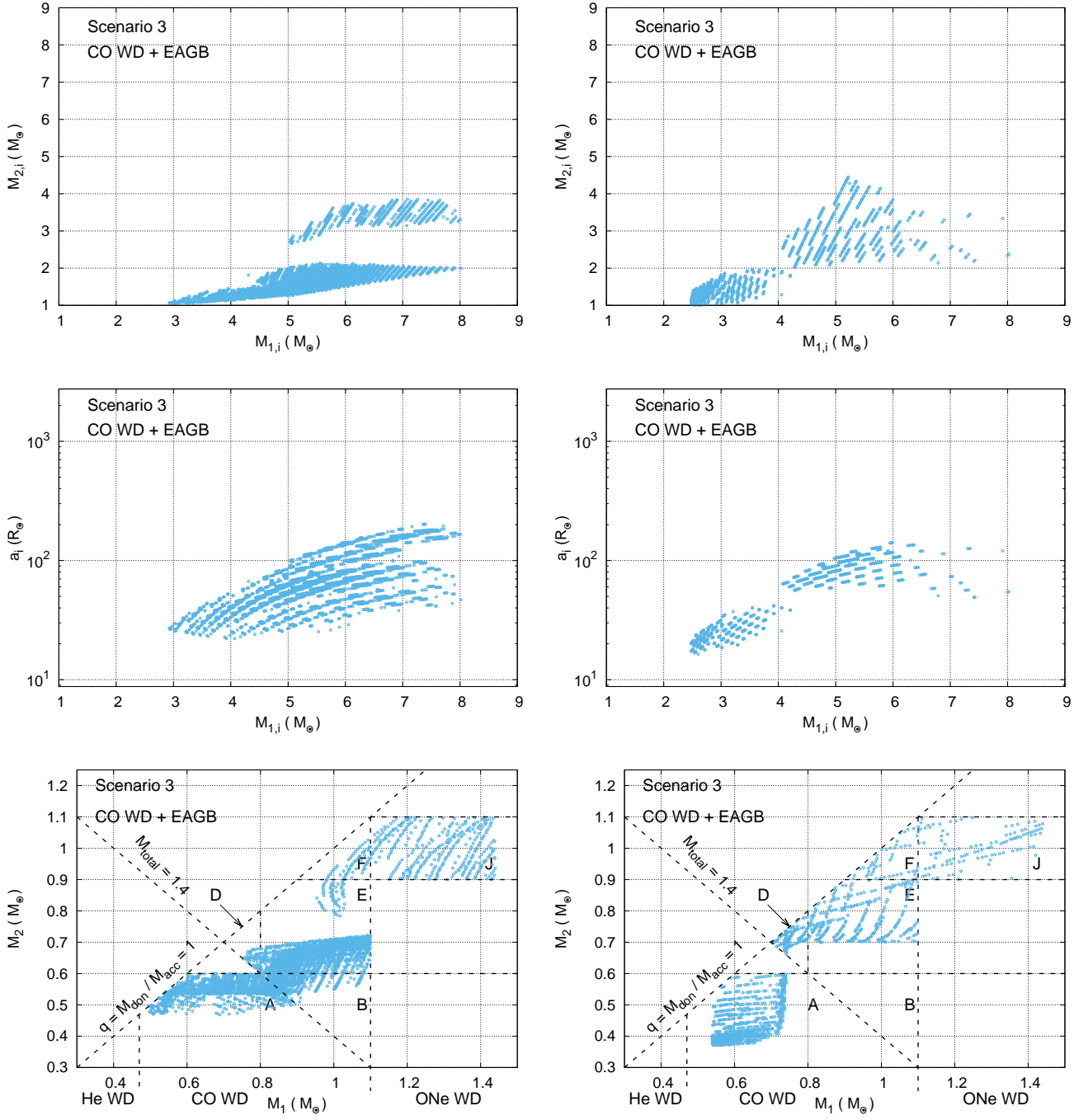


Figure A3. As in Fig. A1, but for scenario 3 with $\alpha_{ce}\lambda=0.25$ (left column) and $\alpha_{ce}\lambda=2$ (right column).

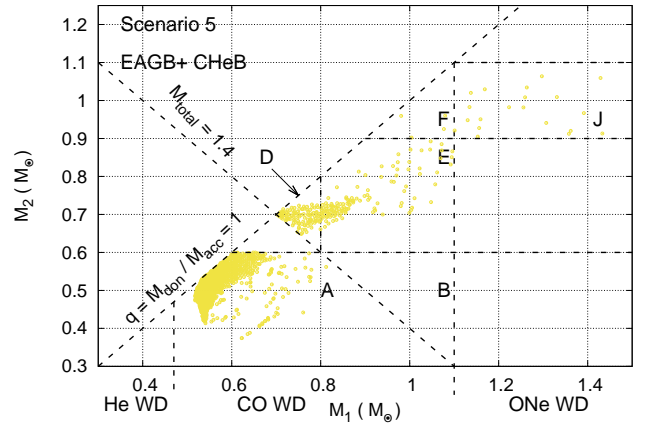
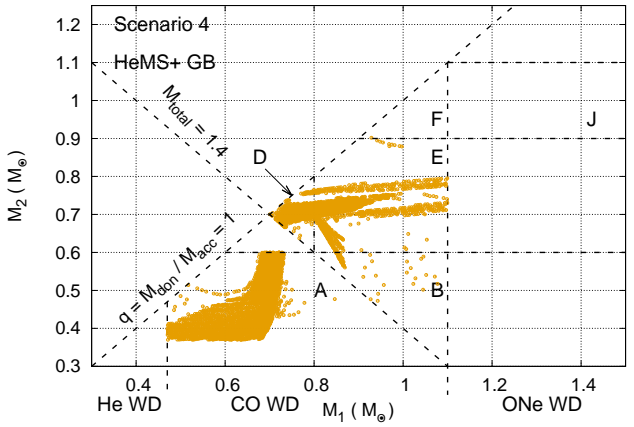
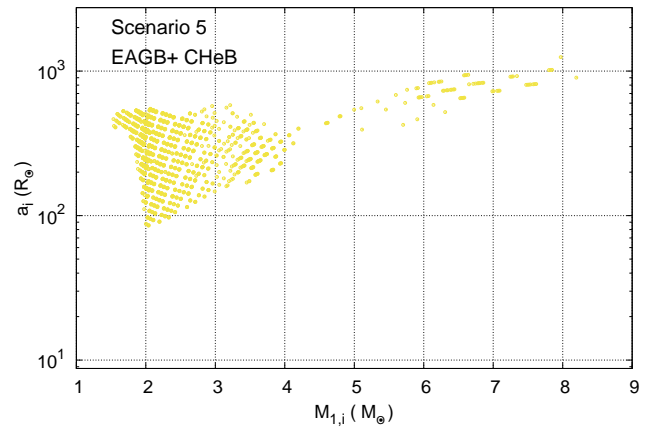
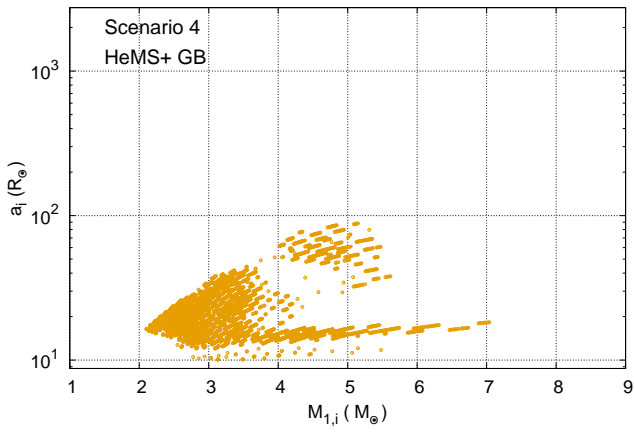
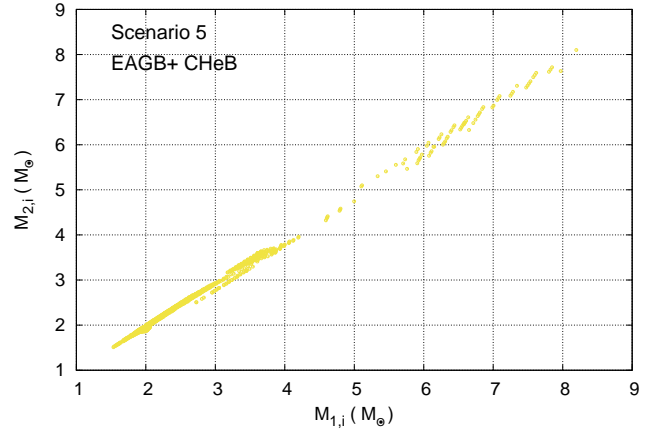
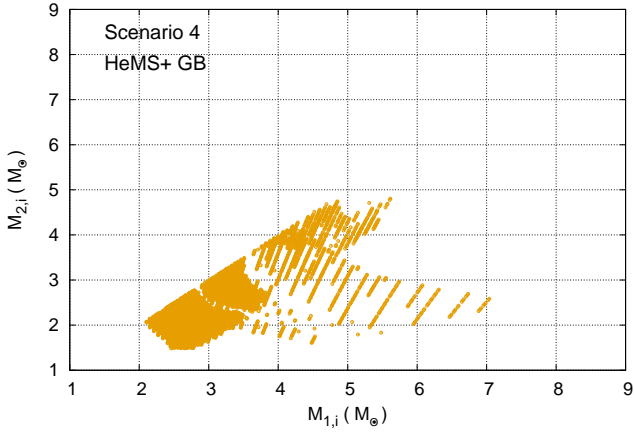


Figure A4. As in Fig. A1, but for scenario 4.

Figure A5. As in Fig. A1, but for scenario 5.

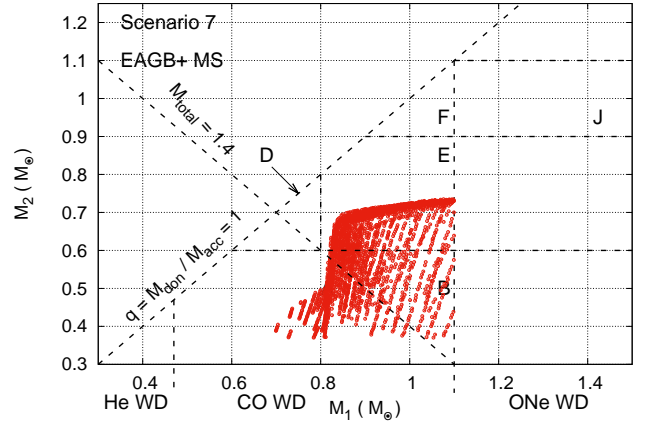
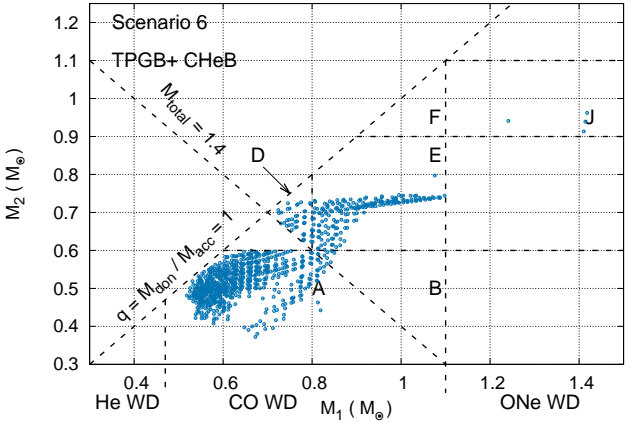
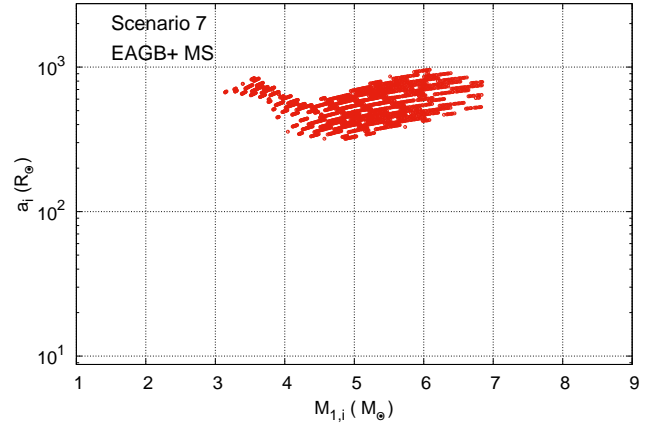
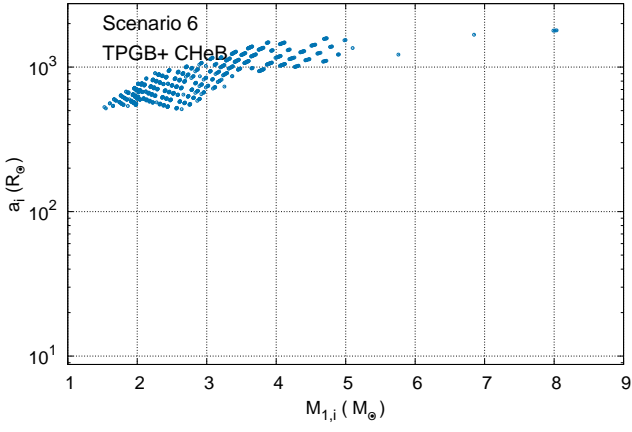
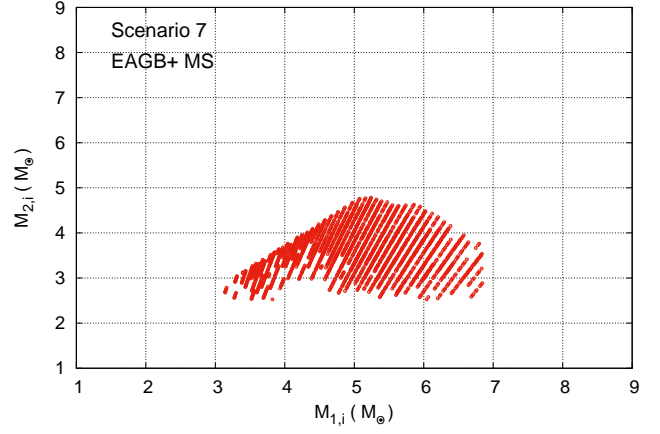
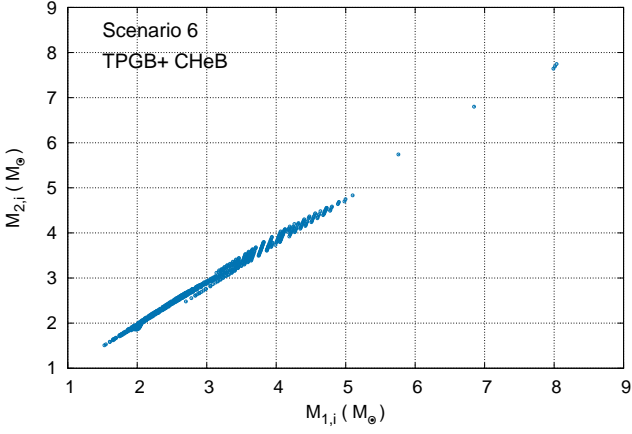


Figure A6. As in Fig. A1, but for scenario 6.

Figure A7. As in Fig. A1, but for scenario 7.

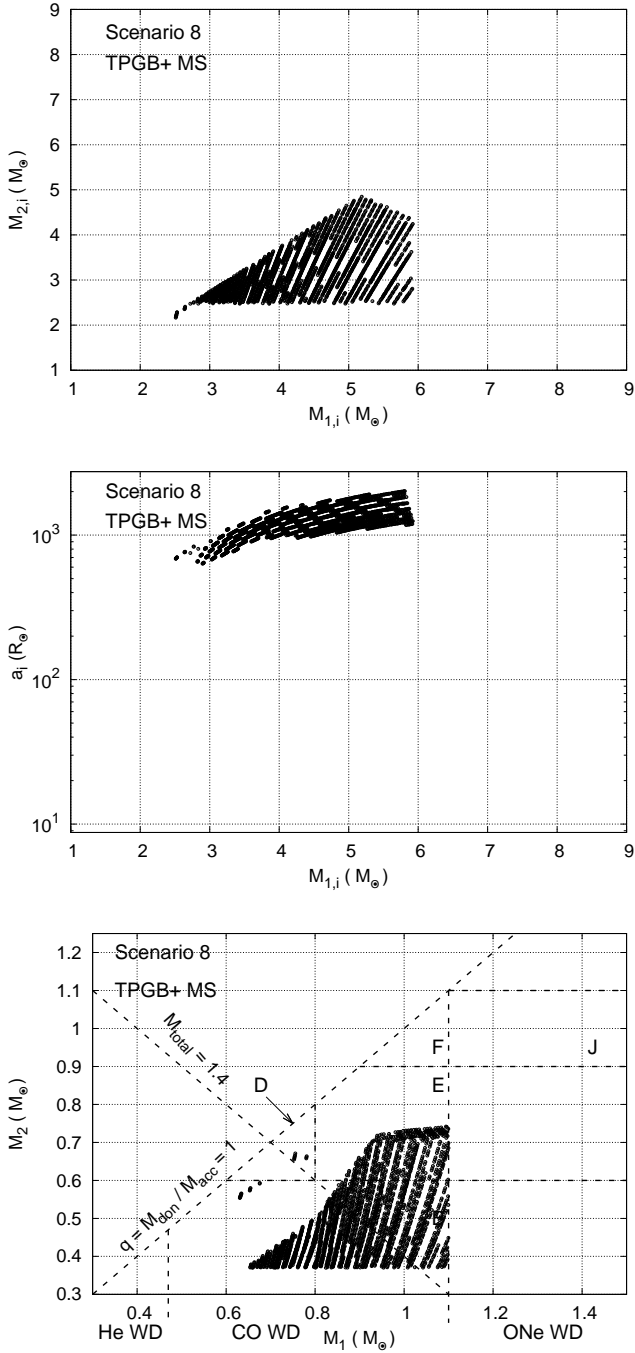


Figure A8. As in Fig. A1, but for scenario 8.

Table A1.

Scenario 1: Formation of a CO WD + CO WD pair							
T (Myr)	Star1	Star2	R1/RL1	R2/RL2	M1	M2	A
0.0	MS	MS	0.36	0.34	4.42	2.06	15.3
139.8	HG	MS	0.83	0.35	4.42	2.06	15.5
139.9	{HG	MS	1.00	0.35	4.42	2.06	15.6
140.5	{GB	MS	1.00	0.09	0.85	4.22	55.5
140.9	HeMS	MS	0.01	0.06	0.72	4.35	72.9
189.4	COHe	MS	0.01	0.08	0.72	4.35	74.0
195.1	COWD	MS	0.001	0.08	0.72	4.35	74.0
276.4	COWD	HG	0.001	0.14	0.72	4.35	74.0
277.1	COWD	HG}	0.001	1.00	0.72	4.35	62.3
			CE				
277.1	COWD	HeMS	0.03	0.39	0.72	0.71	1.06
327.4	COWD	COHe	0.03	0.40	0.72	0.71	1.02
333.2	COWD	COHe}	0.03	1.00	0.72	0.71	1.01
333.3	COWD	COHe	0.03	0.99	0.74	0.69	1.01
333.3	COWD	COWD	0.03	0.03	0.74	0.69	1.01
567.2	COWD	COWD	0.91	1.00	0.74	0.69	0.031
567.2	COWD	COWD	0.91	1.00	0.74	0.69	0.031
567.2	COWD	COWD}	0.91	1.00	0.74	0.69	0.031
							Merger

Table A2.

Scenario 2.1: Formation of a CO WD + He WD pair							
T (Myr)	Star1	Star2	R1/RL1	R2/RL2	M1	M2	A
0	MS	MS	0.29	0.27	3.79	1.34	16.7
204.9	HG	MS	0.65	0.26	3.79	1.34	17.3
205.2	{HG	MS	1.00	0.27	3.79	1.34	17.1
206.2	{GB	MS	1.00	0.06	0.59	2.71	65.0
206.6	HeMS	MS	0.01	0.06	0.59	2.71	65.1
291.5	COHe	MS	0.01	0.06	0.59	2.71	65.7
301.5	COWD	MS	0.00	0.06	0.59	2.71	65.7
687.2	COWD	HG	0.00	0.13	0.59	2.71	65.7
690.3	COWD	GB	0.00	0.35	0.59	2.71	65.8
693.3	COWD	GB}	0.00	1.00	0.59	2.71	48.7
			CE				
693.3	COWD	HeWD	0.03	0.03	0.59	0.40	0.91
1090	COWD	HeWD	0.06	0.08	0.59	0.40	0.57
1165	COWD	HeWD}	0.67	1.00	0.59	0.40	0.05
							Merger
Scenario 2.2: Formation of a CO WD + CO WD pair							
T (Myr)	Star1	Star2	R1/RL1	R2/RL2	M1	M2	A
0	MS	MS	0.20	0.18	4.38	2.34	29
143.4	HG	MS	0.45	0.20	4.38	2.34	29
143.7	{HG	MS	1.00	0.20	4.38	2.34	29
144.4	{GB	MS	1.00	0.03	0.72	4.83	155
144.8	HeMS	MS	0.00	0.03	0.72	4.83	156
193.3	COHe	MS	0.00	0.04	0.71	4.83	159
199.1	COWD	MS	0.00	0.04	0.71	4.83	159
246.3	COWD	HG	0.00	0.07	0.71	4.83	159
246.7	COWD	GB	0.00	0.50	0.71	4.83	160
246.9	COWD	GB}	0.01	1.00	0.71	4.83	107
			CE				
246.9	COWD	HeMS	0.02	0.26	0.71	0.82	1.74
281.4	COWD	COHe	0.02	0.25	0.71	0.82	1.76
285.2	COWD	COHe}	0.02	1.00	0.71	0.82	1.75
285.3	COWD	COWD	0.02	0.02	0.80	0.73	1.75
1972	COWD	COWD}	0.88	1.00	0.80	0.73	0.03
							Merger

Table A3.

Scenario 3.1: Formation of a CO WD + CO WD pair							
T (Myr)	Star1	Star2	R1/RL1	R2/RL2	M1	M2	A
0	MS	MS	0.09	0.08	5.00	2.62	70
103.8	HG	MS	0.20	0.09	5.00	2.62	70
104.2	{HG	MS	1.00	0.09	5.00	2.62	70
104.3	{GB	MS	1.00	0.05	1.70	4.38	124
104.8	HeMS	MS	0.00	0.02	0.87	5.21	337
134.7	COHe	MS	0.00	0.02	0.86	5.21	344
138.2	{COHe	MS	1.00	0.02	0.86	5.21	344
138.3	COWD	MS	0.00	0.02	0.86	5.21	345
189.5	COWD	HG	0.00	0.03	0.86	5.21	345
189.9	COWD	GB	0.00	0.28	0.86	5.21	345
190.1	COWD	CHeB	0.00	0.96	0.86	5.21	242
203.7	COWD	EAGB	0.00	0.71	0.86	5.14	246
203.7	COWD	EAGB}	0.00	1.00	0.86	5.14	180
CE1							
203.7	COWD	COHe	0.01	0.23	0.86	1.25	5.04
203.9	COWD	COHe	0.01	1.00	0.86	1.25	5.03
CE2							
203.9	COWD	COWD	0.02	0.02	0.86	0.75	1.48
956.8	COWD	COWD}	0.84	1.00	0.86	0.75	0.03
Merger							

Scenario 3.2: Formation of a CO WD + CO WD pair							
T (Myr)	Star1	Star2	R1/RL1	R2/RL2	M1	M2	A
0	MS	MS	0.18	0.18	2.83	1.52	24
440.7	HG	MS	0.42	0.19	2.83	1.52	25
442.9	{HG	MS	1.00	0.19	2.83	1.52	24
443.4	{GB	MS	1.00	0.10	1.04	2.51	40
447.8	HeMS	MS	0.00	0.03	0.43	3.12	153
716.2	COHe	MS	0.00	0.05	0.42	3.12	154
743.1	COWD	MS	0.00	0.06	0.42	3.12	154
757.3	COWD	HG	0.00	0.06	0.42	3.12	154
759.3	COWD	GB	0.00	0.19	0.42	3.12	154
761.4	COWD	CHeB	0.00	0.78	0.42	3.12	115
841.0	COWD	EAGB	0.00	0.51	0.42	3.09	116
841.8	COWD	EAGB}	0.00	1.00	0.42	3.09	77
CE							
841.8	COWD	COHe	0.03	0.30	0.42	0.69	1.65
843.7	COWD	COWD	0.03	0.02	0.42	0.69	1.65
4429	{COWD	COWD	1.00	0.60	0.42	0.69	0.05
Merger							

Table A4.

Scenario 4.1: Formation of a CO WD + CO WD pair							
T (Myr)	Star1	Star2	R1/RL1	R2/RL2	M1	M2	A
0	MS	MS	0.13	0.13	3.47	2.48	40
257.6	HG	MS	0.31	0.16	3.47	2.48	40
258.8	{HG	MS	1.00	0.16	3.47	2.48	40
259.0	{GB	MS	1.00	0.10	1.66	4.05	59
267.6	HeMS	MS	0.00	0.02	0.57	5.14	313
337.6	HeMS	HG	0.00	0.04	0.57	5.14	315
338.0	HeMS	GB	0.00	0.28	0.57	5.14	315
338.2	HeMS	GB}	0.00	1.00	0.57	5.14	190
CE							
338.2	HeMS	HeMS	0.18	0.18	0.57	0.90	2.5
351.4	COHe	HeMS	0.15	0.21	0.57	0.89	2.5
362.8	COWD	HeMS	0.02	0.21	0.57	0.89	2.5
366.1	COWD	COHe	0.02	0.18	0.57	0.88	2.5
369.1	COWD	COHe}	0.02	1.00	0.57	0.88	2.5
369.2	COWD	COWD	0.01	0.01	0.71	0.74	2.3
6100	COWD}	COWD	1.00	0.95	0.71	0.74	0.03
Merger							

Scenario 4.2: Formation of a CO WD + ONe WD pair							
T (Myr)	Star1	Star2	R1/RL1	R2/RL2	M1	M2	A
0	MS	MS	0.12	0.11	5.29	4.15	59
91.2	HG	MS	0.27	0.16	5.29	4.15	59
91.4	{HG	MS	1.00	0.16	5.29	4.15	59
91.5	{GB	MS	1.00	0.06	2.06	7.38	123
92.0	HeMS	MS	0.00	0.02	0.93	8.50	449
115.6	HeMS	HG	0.00	0.03	0.92	8.45	462
115.6	HeMS	GB	0.00	0.53	0.92	8.44	463
115.7	HeMS	GB}	0.00	1.00	0.92	8.44	341
CE1							
116.7	COHe	HeMS	0.11	0.14	0.92	1.74	5.5
119.4	{COHe	HeMS	1.00	0.15	0.92	1.72	5.6
119.5	COHe	HeMS	0.80	0.12	0.78	1.86	6.7
119.5	COWD	HeMS	0.01	0.12	0.78	1.86	6.7
121.5	COWD	COHe	0.01	0.10	0.78	1.82	6.9
122.0	COWD	COHe}	0.01	1.00	0.78	1.82	7.0
CE2							
122.0	COWD	ONeWD	0.02	0.01	0.78	1.04	1.44
592	{COWD	ONeWD	1.00	0.63	0.78	1.04	0.03
Merger							

Table A5.

Scenario 5: Formation of a CO WD + CO WD pair							
T (Myr)	Star1	Star2	R1/RL1	R2/RL2	M1	M2	A
0	MS	MS	0.03	0.03	2.30	2.29	177
785	HG	MS	0.06	0.07	2.30	2.29	177
791	GB	MS	0.12	0.07	2.30	2.29	177
793	GB	HG	0.14	0.06	2.30	2.29	177
799	GB	GB	0.39	0.12	2.30	2.29	175
800	CHeB	GB	0.48	0.12	2.30	2.29	174
808	CHeB	CHeB	0.18	0.49	2.29	2.29	172
1011	EAGB	CHeB	0.33	0.29	2.27	2.27	177
1014	{EAGB	CHeB	1.00	0.32	2.27	2.27	168
CE							
1016	COWD	HeMS	0.03	0.28	0.57	0.56	1.24
1105	COWD	COHe	0.03	0.27	0.57	0.55	1.22
1117	COWD	COWD	0.03	0.03	0.57	0.55	1.22
2121	COWD	COWD}	0.98	1.00	0.57	0.55	0.04
Merger							

Table A6.

Scenario 6: Formation of a CO WD + CO WD pair							
T (Myr)	Star1	Star2	R1/RL1	R2/RL2	M1	M2	A
0	MS	MS	0.00	0.00	3.60	3.38	1351
234.3	HG	MS	0.01	0.01	3.60	3.38	1351
235.5	GB	MS	0.04	0.01	3.60	3.38	1351
236.6	CHeB	MS	0.12	0.01	3.60	3.38	1352
275.4	CHeB	HG	0.06	0.01	3.57	3.38	1365
276.9	CHeB	GB	0.06	0.04	3.57	3.38	1366
278.3	CHeB	CHeB	0.07	0.11	3.57	3.38	1367
283.8	EAGB	CHeB	0.08	0.05	3.57	3.37	1375
285.8	TPAGB	CHeB	0.66	0.05	3.53	3.38	1359
286.3	{TPAGB	CHeB	1.00	0.05	3.34	3.41	1362
		CE					
286.3	COWD	HeMS	0.02	0.36	0.81	0.55	1.02
387.5	COWD	COHe	0.03	0.39	0.81	0.55	0.91
400.0	COWD	COWD	0.03	0.04	0.81	0.55	0.89
567.6	COWD	COWD}	0.63	1.00	0.81	0.55	0.04
		Merger					

Table A7.

Scenario 7: Formation of a CO WD + CO WD pair							
T (Myr)	Star1	Star2	R1/RL1	R2/RL2	M1	M2	A
0	MS	MS	0.02	0.01	4.86	4.08	449
111.3	HG	MS	0.03	0.02	4.86	4.08	449
111.7	GB	MS	0.25	0.02	4.86	4.08	449
112.0	CHeB	MS	0.64	0.02	4.86	4.08	437
128.9	EAGB	MS	0.46	0.03	4.80	4.08	444
129.5	{EAGB	MS	1.00	0.03	4.79	4.08	426
		CE1					
129.5	COHe	MS	0.42	0.20	1.15	4.08	41
129.5	COHe	MS	1.00	0.20	1.15	4.08	41
129.6	COWD	MS	0.00	0.12	0.86	4.37	64
171.3	COWD	HG	0.00	0.17	0.86	4.37	64
171.9	COWD	HG}	0.00	1.00	0.86	4.37	60
		CE2					
171.9	COWD	HeMS	0.02	0.37	0.86	0.72	1.18
221.5	COWD	COHe	0.02	0.38	0.86	0.71	1.14
227.2	COWD	COHe}	0.02	1.00	0.86	0.71	1.13
227.3	COWD	COWD	0.02	0.03	0.88	0.69	1.15
518.6	COWD	COWD}	0.73	1.00	0.88	0.69	0.03
		Merger					

Table A8.

Scenario 8.1: Formation of a CO WD + CO WD pair							
T (Myr)	Star1	Star2	R1/RL1	R2/RL2	M1	M2	A
0	MS	MS	0.01	0.01	3.97	3.30	1198
182.4	HG	MS	0.01	0.01	3.97	3.30	1198
183.3	GB	MS	0.06	0.01	3.97	3.30	1198
184.0	CHeB	MS	0.16	0.01	3.97	3.30	1198
217.2	EAGB	MS	0.11	0.01	3.93	3.30	1216
218.7	TPAGB	MS	0.76	0.01	3.89	3.31	1177
219.0	{TPAGB	MS	1.00	0.01	3.80	3.32	1158
		CE1					
219.0	COWD	MS	0.00	0.07	0.85	3.32	104
291.7	COWD	HG	0.00	0.09	0.85	3.32	104
293.3	COWD	GB	0.00	0.36	0.85	3.32	104
294.6	COWD	GB}	0.00	1.00	0.85	3.32	80
		CE2					
294.6	COWD	HeMS	0.01	0.19	0.85	0.51	1.804
436.4	COWD	COHe	0.01	0.19	0.85	0.50	1.791
452.4	COWD	COWD	0.01	0.02	0.85	0.50	1.786
3288	COWD	COWD}	0.54	1.00	0.85	0.50	0.042
		Merger					

Scenario 8.2: Formation of a CO WD + CO WD pair							
T (Myr)	Star1	Star2	R1/RL1	R2/RL2	M1	M2	A
0	MS	MS	0.01	0.01	3.26	2.94	1093.7
303.5	HG	MS	0.01	0.01	3.26	2.94	1093.7
305.2	GB	MS	0.04	0.01	3.26	2.94	1093.8
306.9	CHeB	MS	0.13	0.01	3.26	2.94	1094.3
374.7	EAGB	MS	0.08	0.01	3.23	2.94	1108.5
377.3	TPAGB	MS	0.64	0.01	3.20	2.95	1094.0
377.9	{TPAGB	MS	1.00	0.01	3.04	2.97	1097.3
		CE1					
377.9	COWD	MS	0.00	0.08	0.75	2.97	120.0
396.6	COWD	HG	0.00	0.08	0.75	2.97	120.0
398.9	COWD	GB	0.00	0.24	0.75	2.97	120.0
401.5	COWD	CHeB	0.00	0.98	0.75	2.97	93.5
495.7	COWD	EAGB	0.00	0.64	0.76	2.95	94.5
496.6	COWD	EAGB}	0.00	1.00	0.76	2.94	76.5
		CE2					
496.6	COWD	COHe	0.01	0.19	0.76	0.67	2.8
498.8	COWD	COWD	0.01	0.01	0.76	0.67	2.8
13225	COWD	COWD}	0.86	1.00	0.76	0.67	0.03
		Merger					